J, Kim DY, Inoue T, Hirabayashi Y: Mechanisms of benzene-induced hematotoxicity and leukemogenicity cDNA microarray analyses using mouse bone marrow tissue. Env Health Perspect (Toxicogenomics), 111: 1411-1420, 2003

* Yoshimura K, Sakurai Y, Nishimura D, Tsuruo Y, Nomura M, Kawato S, Seiwa C, Iguchi T, Itoh K, Asou H: Monoclonal antibody 14F7, which recognizes a stage-specific immature oligodendrocyte surface molecule, inhibits oligodendrocyte differentiation mediated in co-culture with astrocytes. J Neurosci Res, 54: 79-96, 1998

* Zhou J, Suzuki T, Kovacic A, Saito R, Miki Y, Ishida T, Moriya T, Simpson ER, Sasano H, Clyne CD: Interactions between prostaglandin E(2), liver receptor homologue-1, and aromatase in breast cancer. Cancer Res, 65: 657-663, 2005

TOXICOLOGICAL SCIENCES 80, 161–169 (2004)
DOI: 10.1093/toxsci/kfh129
Advance Access publication March 31, 2004

Comparison of Gene Expression Patterns between 2,3,7,8-Tetrachlorodibenzo-*p*-dioxin and a Natural Arylhydrocarbon Receptor Ligand, Indirubin

Jun Adachi,* Yoshitomo Mori,† Saburo Matsui,* and Tomonari Matsuda,*,[1]

*Department of Technology and Ecology, Graduate School of Global Environmental Studies, Kyoto University, Kyoto, Japan, and †Japanese Ministry of the Environment, Tokyo, Japan

Received December 26, 2003; accepted March 10, 2004

Indirubin is a natural arylhydrocarbon receptor (AhR) ligand isolated from human urine. We previously reported that it was more potent than the prototypical ligand, 2,3,7,8-tetrachlorodibenzo-*p*-dioxin (TCDD) in a yeast assay system. Here we compared gene expression changes in HepG2 cells exposed to 10 nM of indirubin or TCDD using nylon-membrane-based cDNA arrays with 1176 genes to elucidate the toxic differences at the transcriptional level. The gene expression profiles for TCDD and indirubin were very similar. The number of up-regulated genes (fold change ≥2.0) was 11 and 4 and the number of down-regulated genes (fold change ≤0.5) was 17 and 21 in TCDD-treated and indirubin-treated cells, respectively. Cytochrome P450 (CYP) 1A1, 1A2, 19A1, insulin-like growth factor binding protein 1 (IGFBP1), and IGFBP10 were confirmed to be up-regulated using real-time reverse transcription polymerase chain reaction. CYP1A1 and CYP1A2 mRNAs were induced by as little as 1 pM of indirubin, whereas they were not induced by 10 pM of TCDD. In the time-course experiment, CYP1A1 mRNA was induced by indirubin transiently. Indirubin was also metabolized by CYP1A1 and lost its ligand activity. Indirubin would appear to be a good substrate of CYP1A1 given its low dissociation constant. Our results suggest that indirubin rapidly activates its own metabolism via AhR-mediated induction of CYP1A1 and this characteristic is consistent with the notion that indirubin is a physiological ligand of AhR.

Key Words: indirubin; AhR; TCDD; CYP1A1; metabolism; gene expression.

Arylhydrocarbon receptor (AhR) is a ligand-activated transcription factor that is present in most cells and tissue types of the body (Pohjanvirta and Tuomisto, 1994) and mediates most, if not all, toxic and biological effects of dioxins in various species and tissues (Fernandez-Salguero *et al.*, 1995, 1996; Lucier *et al.*, 1993; Mimura *et al.*, 1997). The ligand-bound AhR forms a heterodimer with Ah receptor nuclear translocator (ARNT) and activates the transcription of the Ah gene battery which includes cytochrome P450 1A1 (CYP1A1), 1A2 (CYP1A2), glutathione S-transferase Ya subunit (GSTA1, Ya), NAD(P)H: quinone oxidoreductase (NQO1), UDP-glucuronosyltransferase 1A6 (UGT1A6), and aldehyde-3-dehydrogenase 3 (ALDH3A1) genes (Nebert *et al.*, 2000). In addition, the prototypical AhR ligand, 2,3,7,8-tetrachlorodibenzo-*p*-dioxin (TCDD), has been reported to modulate the expression of genes for protein kinase C (PKC) family (Moore *et al.*, 1993; Puga *et al.*, 2000), estrogen receptor (Lu *et al.*, 1994), several cytokines such as interleukin-1β (IL-1β; Gaido and Maness, 1994), IL-2 (Jeon and Esser, 2000), tumor growth factor-β2 (TGF-β2; Vogel and Abel, 1995) and tumor necrosis factor-α (TNF-α; Vogel and Abel, 1995), cyclooxygenase isoenzymes COX-1 and COX-2 (Puga *et al.*, 1997; Wolfle *et al.*, 2000), the immediately-early proto-oncogenes c-fos and c-jun (Puga *et al.*, 1992), and tumor suppressor p27 (Kolluri *et al.*, 1999).

We previously reported that indirubin was more potent than TCDD in inducing transactivation of a reporter gene in yeast that expressed human AhR and ARNT proteins (Adachi *et al.*, 2001). Indirubin was also proved to be a high (K_d = 12.2 nM) affinity AhR ligand by competitive binding assay using rat liver cytosol and [^{3}H]TCDD (Rannug *et al.*, 1992). Indirubin is a pink colored pigment and synthesized as a by-product of indigo (Fig. 1). Indirubin's bioactivity has been studied because it is also an active component of the Chinese traditional medicine, Danggui Longhui Wan, which is used to cure chronic myelocytic leukemia (CML). Indirubin is a potent inhibitor of cyclin-dependent kinases (CDKs) and of glycogen synthase kinase-3β (GSK-3β), which may play an important role in the development of Alzheimer's disease (Hoessel *et al.*, 1999). It also inhibits inflammation in delayed-type hypersensitivity reactions (Kunikata *et al.*, 2000). Furthermore, indirubin was confirmed to be a product of the human cytochrome P450-catalyzed metabolism of indole, a product of the tryptophan catabolite (Gillam *et al.*, 2000). We have previously detected indirubin in human urine of healthy individuals and in fetal bovine serum at average

A portion of this article was previously published in the 22nd International Symposium on Halogenated Environmental Organic Pollutants and POPs (2002) 56, 13–15 and the 2nd Pacific Conference on Reproductive Biology and Environmental Sciences (2002) 35–37.

[1]To whom correspondence should be addressed at Department of Technology and Ecology, Graduate School of Global Environmental Studies, Kyoto University, Yoshida-honmachi, Sakyo-ku, Kyoto 606-8501, Japan. Fax: + 81-75-753-5171. E-mail: matsuda@eden.env.kyoto-u.ac.jp.

concentrations of 0.2 and 0.07 nM, respectively (Adachi *et al.*, 2001). Both indirubin and TCDD are potent AhR ligands. But TCDD has pleiotropic toxicity while indirubin seems to be non-toxic since it is excreted into our urine everyday. To elucidate this toxic difference, the present study was undertaken to compare the gene expression profiles and metabolism of the potent natural AhR ligand, indirubin, with those of the prototypical AhR ligand, TCDD.

MATERIALS AND METHODS

Materials. Analytical grade chemicals were purchased from Wako (Osaka, Japan). Microsomes from baculovirus-infected insect cells coexpressing NADPH-cytochrome P450 reductase and human CYP1A1 and control insect cell microsomes were purchased from BD Gentest (Wobum, MA). Indirubin was synthesized as described previously (Hoessel *et al.*, 1999) and kindly provided by Dr. Saeki (Nagoya City University, Nagoya, Japan). The purity of indirubin was confirmed by HPLC.

Cell culture and treatments. The human hepatocarcinoma cell line HepG2 was obtained from the Cell Resource Center for Biomedical Research, Institute of Development, Aging and Cancer, Tohoku University, Japan. The cells were grown at 37°C in air supplemented with 5% CO_2. Cells cultured in Dulbecco's modified Eagle's medium supplemented with 10% fetal bovine serum were seeded into 10-cm dishes (4×10^6 cells/dish) containing fresh medium and 24 h later (70–80% confluence) exposed to the test chemicals. The chemicals were dissolved in DMSO and added to the medium directly. The final DMSO concentration was 1.0% (v/v).

Gene expression arrays. HepG2 cells were exposed to 10 nM of indirubin or TCDD for 8 h and subsequently total RNA was isolated with RNeasy Mini Kit (Qiagen, Hilden, Germany). RNA quality and quantity were assessed using agarose gel electrophoresis and spectrophotometric absorbency at 260/280 nm. Using 50 μg of total RNA, poly $(A)^+$ RNA enrichment and radiolabeled cDNA probe synthesis were carried out using an Atlas Pure Total RNA Labeling System (Clontech, Palo Alto, CA). The ^{33}P-labeled cDNA probes were separated from unincorporated nucleotides and small cDNA fragments by using a spin column (Atlas Nucleo Spin Extraction Kit, Clontech). We used Clontech Atlas human 1.2-toxicology microarrays with 1176 genes per array. Clontech Atlas arrays are nylon-membrane-based cDNA arrays used for broadscale differential gene expression profiling. The human 1.2-toxicology array contains genes associated with xenobiotic metabolism, drug resistance, stress response, apoptosis, cell cycle, cell surface antigens, transcriptional activation, oncogenes, cytokines, signal transduction, cytoskeleton, energy metabolism, and DNA metabolism.

Purified ^{33}P-labeled cDNA probes were hybridized with the array and the array was washed according to the manufacturer's instructions. Arrays were placed on an imaging plate (Fuji, Tokyo, Japan) for one week and visualized using a bioimaging analyzer (FLA-2000, Fuji). Image files were imported into AtlasImage 2.01 (CLONTECH) for quantification. Each data point was normalized to the total intensity of the array filter (the sum of signal values over the background for all genes on the filter) by using the "global normalization" feature in AtlasImage 2.01. An intensity ratio (treated/control) threshold value of 2 for up-regulation and 0.5 for down-regulation was used in an attempt to detect significant changes in expression.

Real-time RT-PCR. To confirm the results of the microarray analysis, the expression of some genes was analyzed by real-time RT-PCR. Total RNA was extracted as described previously. cDNA was synthesized from 100 ng of total RNA using RNA PCR Kit (AMV) Ver.2.1(Takara, Shiga, Japan) as the manufacturer instructed. Synthesized cDNA (2 μl) was amplified in a total volume of 25 μl containing 0.3 mM dNTP, 50 mM KCl, 3.4 mM $MgCl_2$, 1 μl of SYBR Green (1000 × diluted, Cambrex, Rockland, ME), 1.25 U of *TaKaRa Ex Taq* R-PCR version (Takara), and 0.2 μM of each primer. Primer sequences are listed in Table 1. PCR was performed using a Smart Cycler (Cepheid, Sunnyvale, CA). After 30 s denaturation at 94°C, PCR was carried out for 40 cycles with denaturation at 94°C for 3 s, annealing and extension at 60°C for 30 s. All signals were normalized against actin beta mRNA as a control.

TABLE 1
RT-PCR Primers

Gene	Primer sequence	Size (bp)
IGFBP1	5′-CCCAGAGAGCACGGAGATAA-3′ 5′-TATCTGGCAGTTGGGGTCTC-3′	391
IGFBP10	5′-CAACCCTTTACAAGGCCAGA-3′ 5′-TGTAGAAGGGAAACGCTGCT-3′	449
CYP19A1	5′-CACTGGCCTTTTTCTCTTGG-3′ 5′-AGAAGGGTCAACACGTCCAC-3′	480
Actin beta	5′-AGAAAATCTGGCACCACACC-3′ 5′-CCATCTCTTGCTCGAAGTCC-3′	435
CYP1A1	[a] [a]	433
CYP1A2	[a] [a]	309

[a]These primers are contained in the human cytochrome P450 competitive RT-PCR set (Takara, Shiga, Japan). The sequences of the primers are not available for proprietary reasons.

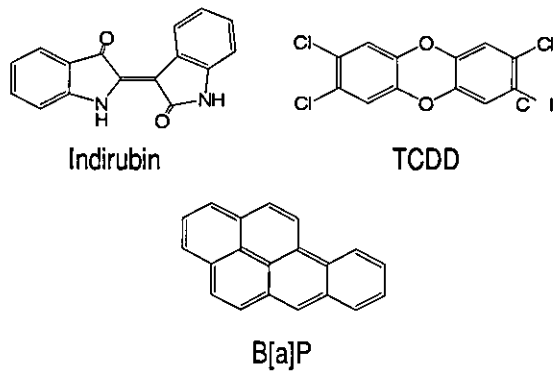

FIG. 1. Molecular structures of indirubin, TCDD, and B[a]P.

Competitive RT-PCR. Total RNA was isolated as mentioned above. Quantitative competitive RT-PCR for CYP1A1, CYP1A2, CYP2C, CYP2D6, and CYP2E1 mRNA was carried out using a human cytochrome P450 competitive RT-PCR set and RNA PCR Kit (AMV) Ver. 2.1 (Takara) as instructed. With this method, target mRNA and appropriate copies of competitor RNA are mixed and reverse transcribed. Target cDNA and competitor cDNA share the same primer to be amplified and are separated by electrophoresis because the amplified genes differ in length. The ratio of target band to competitor band is equal to the ratio of target mRNA copies to competitor RNA copies, thus one can know the number of target mRNA copies from the known number of competitor RNA copies. The competitor RNA is designed to contain competitive primers' sequences to amplify all target genes (CYP1A1, 1A2, 2C, 2D6, 2E1, and GAPDH). The sequences of the primers and competitor RNA are not available for proprietary reasons. The PCR reaction mixtures were heated to 94°C for 2 min and immediately cycled through 30 s of denaturing at 94°C, 60 s of annealing at 60°C and

60 s of extension step 72°C. The reaction comprised 33 cycles for the CYP1A1 gene, 38 cycles for the CYP1A2 gene, 40 cycles for the CYP2A6, 2C, 2D6, and 2E1 genes, and 28 cycles for the GAPDH gene. After the amplification, PCR products (5 μl) were separated on a 2.5% agarose gel and visualized by ethidium bromide staining. Images were captured digitally using a Kodak Electrophoresis Documentation and Analysis System (EDAS) 290LE (Eastman Kodak, Rochester, NY) and the bands were quantified using NIH image program. All signals were normalized to GAPDH mRNA as a control.

Indirubin metabolism by CYP1A1. Four types of reaction mixtures were made. Reaction mixture 1 contained 15 pmol of recombinant CYP1A1 enzyme, 4 mM NADPH, and 3.3 mM $MgCl_2$ in 0.1 M sodium-potassium phosphate buffer (pH 7.4). Reaction mixture 2 was the same except that it contained 15 pmol of control microsomes instead of CYP1A1 and had 100 nM indirubin. Reaction mixture 3 was equivalent to mixture 1 except that it had 100 nM indirubin and lacked NADPH. Reaction mixture 4 was the same as mixture 1 but it included 100 nM indirubin. Each reaction mixture (100 μl) was incubated at 37°C for 3 h. Then 1 μl of the mixture was subjected to a yeast assay. The yeast assay was performed essentially as described previously (Adachi *et al.*, 2001; Miller, 1999). In the yeast strain YCM3, human AhR and ARNT genes are integrated into chromosome III. AhR and ARNT are expressed from the galactose-regulated GAL 1, 10 promoter. Ligand-dependent activation of AhR leads to formation of the AhR/ARNT heterodimer. Expression of the lacZ reporter plasmid is directed by the AhR/ARNT complex binding to five xenobiotic response elements (XREs) in the promoter region. Thus, AhR ligand activity can be detected and quantified by measuring β-galactosidase activity.

Measuring the dissociation constant of AhR ligands. The 7-ethoxyresorufin *O*-deethylation activity of the recombinant human CYP1A1 was determined by a continuous spectrofluorometric method as described previously (Chang *et al.*, 2001), but with minor modifications. Briefly, the general reaction mixture, prepared in a spectrofluorimetric cuvette, contained 2 ml of sodium-potassium phosphate buffer (0.1 M, pH 7.4), 7-ethoxyresorufin (ranging from 0.1 μM to 1.0 μM), 50 μM NADPH, 2.5 pmol human recombinant CYP1A1 enzyme and the inhibitor at the concentration indicated in each figure. The reaction was run at 30°C. A baseline of fluorescence was recorded at an excitation wavelength of 510 nm and an emission wavelength of 586 nm. Calibration curves were constructed with a resorufin standard and a linear regression analysis was used to calculate the amount of resorufin formed in each incubation sample. The K_i values were determined according to a previously described procedure (Chang *et al.*, 2001).

RESULTS

Indirubin and TCDD-Responsive Genes

Changes of gene expression were analyzed using Atlas human 1.2-toxicology microarray (CLONTECH) with 1176 genes per array in order to characterize the effect of indirubin and TCDD on human hepatocarcinoma HepG2 cells. Table 2 shows the differential gene expression profiles of TCDD-treated and indirubin-treated cells. The number of up-regulated genes (fold change ≥ 2.0) in TCDD-treated and indirubin-treated cells were 11 and 4, respectively. The CYP1A1 gene was prominently up-regulated, 446-fold in TCDD-treated cells and 88 fold in indirubin-treated cells. Other up-regulated genes were IGFBP10, GSTP1, CYP19A1, IGFBP1, NPC1, CYP1A2, SOX9, EGR1, IGF2, and CDKN1A. The number of down-regulated genes (fold change ≤0.5) in TCDD-treated and indirubin-treated cells was 17 and 21, respectively. We further analyzed the mRNA levels of CYP1A1, CYP1A2, CYP19A1, IGFBP1, and IGFBP10 by real-time RT-PCR to confirm the finding of the cDNA microarray analysis (Table 2). As shown in Figure 2, CYP19A1, IGFBP1, and IGFBP10 mRNA were induced by indirubin dose-dependently.

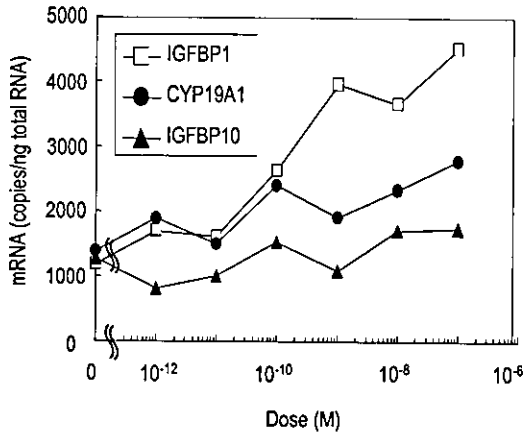

FIG. 2. Effect of indirubin on CYP19A1, IGFBP1, and IGFBP10 mRNA levels in HepG2 cells. HepG2 cells (4×10^6) were seeded into 10-cm dishes, and 24 h later a stock solution of indirubin or DMSO (control) was added to the medium. After 8 h, total RNA was extracted and CYP19A1, IGFBP1, and IGFBP10 mRNA expression was quantified by real-time RT-PCR. Each dot represents the average obtained from two separate experiments.

Dose-Response and Time Course Changes of CYP1A mRNA Induced by Indirubin, TCDD, and B[a]P

We examined the expression of CYP1A1 and 1A2 mRNA induced by AhR ligands, indirubin, TCDD and benzo[a]pyrene (B[a]P) in HepG2 cells. Since fetal bovine serum is known to contain endogenous AhR ligands (Guigal *et al.*, 2001), we measured the CYP1A1 mRNA level without adding any test chemicals. At 8 h after the change of medium, CYP1A1 mRNA level was 2550 copies/ng total RNA. But at 32 h, the level had dropped to 100 copies/ng total RNA. Therefore, we allowed a 24 h period between cell seeding and chemical exposure to lower the background level. This operation made it possible to observe CYP1A mRNA induction at very low concentrations.

Figure 3A shows that 1 pM of indirubin significantly induced CYP1A1 mRNA expression (9.4-fold) after 8 h exposure. The expression was induced by indirubin, TCDD, and B[a]P in a dose-dependent manner (Fig. 3B). The indirubin dose-response curve was different from the TCDD dose-response curve in that it was not sigmoid in shape. The mRNA expression was relatively constant for the treatments with 1 pM to 1 nM of indirubin. These doses of indirubin were associated with ~1000–2000 copies CYP1A1 mRNA/ng total RNA (10–20 copies/cell). These levels were significantly higher than the control level (1 copy/cell) ($p < 0.01$). When cells were exposed to 100 nM of indirubin, we observed ~7900 copies of CYP1A1 mRNA/ng RNA (~79 copies/cell). In contrast, TCDD did not induce CYP1A1 mRNA expression significantly at a concentration

TABLE 2
Differential Gene Expression Profiles of TCDD-Treated Cells and Indirubin-Treated Cells

GeneBank no.	Gene name	TCDD (10 nM)		Indirubin (10 nM)	
		Array results[a]	RT-PCR results[a]	Array results[a]	RT-PCR results[a]
K03191	Cytochrome P450 1A1 (CYP1A1)	446	144	88.0	64.6
AF031385	Insulin-like growth factor-binding protein 10 (IGFBP10)	7.0	9.4	3.8	1.4
X08058	Glutathione S-transferase pi (GSTP1)	5.3		2.0	
M22246	Cytochrome P450 19A1 (CYP19A1)	4.3	7.0	1.9	2.5
M31145	Insulin-like growth factor binding protein 1 (IGFBP1)	4.2	9.7	1.6	3.7
AF002020	Niemann-Pick C disease protein (NPC1)	2.8		2.2	
Z00036	Cytochrome P450 1A2 (CYP1A2)	2.6	10.0	1.5	4.6
Z46629	Sex-determining region Y box-containing gene 9 (SOX9)	2.3		1.3	
X52541	Early growth response protein 1 (EGR1)	2.3		1.5	
M29645	Insulin-like growth factor II (IGF2)	2.2		1.4	
L25610	Cyclin-dependent kinase inhibitor 1A (CDKN1A); $p21^{waf1}$	2.2		1.1	
M80627	Transcription factor HTF4; transcription factor 12 (TCF12)	0.32		0.40	
J03810	Solute carrier family 2 member 2 (SLC2A2)	0.34		0.45	
D86956	110-kDa heat-shock protein (HSP110)	0.35		0.43	
AF068754	Heat shock factor-binding protein 1 (HSBP1)	0.38		0.46	
M15353	Eukaryotic translation initiation factor 4E 25-kDa subunit (EIF4E)	0.39		0.53	
M96577	Retinoblastoma-binding protein 3 (RBBP3)	0.41		0.36	
U77604	Microsomal glutathione S-transferase 2 (MGST2)	0.41		0.49	
M34664	Heat shock 60-kDa protein (HSP60)	0.43		0.48	
L34587	RNA polymerase II elongation factor SIII p15 subunit	0.43		0.62	
X05360	Cyclin-dependent kinase 1 (CDK1)	0.45		0.46	
Z30093	Basic transcription factor 2 34-kDa subunit (BTF2p34)	0.46		0.59	
M65134	Complement component 5 (C5)	0.47		0.57	
D13627	T-complex protein 1 theta subunit (TCP1-theta)	0.48		0.58	
X07979	Integrin beta 1 (ITGB1)	0.48		0.44	
U38846	T-complex protein 1 delta subunit (TCP1-delta)	0.49		0.42	
Y08201	Rab geranylgeranyl transferase beta subunit	0.49		0.54	
AF054184	Sec61-gamma (SEC61G)	0.49		0.76	
M36341	ADP ribosylation factor 4 (ARF4)	0.52		0.49	
AF084260	Thyroid receptor-interacting protein 15 (TRIP15)	0.58		0.46	
J04088	DNA topoisomerase II alpha (TOP2A)	0.60		0.44	
D63878	NEDD5 protein homolog; DIFF6	0.60		0.38	
M27492	Interleukin 1 receptor type I (IL1R1)	0.65		0.44	
U12778	Short/branched chain-specific acyl-CoA dehydrogenase (SBCAD; ACADSB)	0.65		0.49	
U04045	DNA mismatch repair protein (MSH2)	0.66		0.47	
J03250	DNA topoisomerase I (TOP1)	0.68		0.41	
M34064	Cadherin 2 (CDH2)	0.70		0.45	
U10323	45-kDa Interleukin enhancer-binding factor 2 (ILF2)	0.72		0.28	
L29222	CDC-like kinase 1 (CLK1)	1.4		0.32	

Note. Fold change represents the ratio of treated/control. Fold change threshold values of 2 for up-regulation and 0.5 for down-regulation were used in an attempt to detect significant changes in expression.

[a]Array results and RT-PCR results are presented as fold change.

of 10 pM. But the expression level elevated sharply at a concentration over 100 pM. One nM of TCDD induced ~32,000 copies of CYP1A1 mRNA/ng total RNA (~320 copies/cell). Another AhR ligand, B[a]P, induced CYP1A1 mRNA expression at a concentration over 100 nM.

As shown in Figure 3C, indirubin induced CYP1A2 mRNA as well as CYP1A1 mRNA expression. The background level of CYP1A2 mRNA was 10–16 copies/ng total RNA (0.1–0.16 copies/cell). At 1 pM, indirubin significantly induced the expression (0.67 copies/cell) ($p < 0.01$), and the level increased up to 1 nM (1.6 copies/cell). TCDD and B[a]P also induced CYP1A2 mRNA expression in a dose-dependent manner, but they were less potent than indirubin.

The time course of CYP1A1 mRNA induction by indirubin, TCDD, and B[a]P, is shown in Fig. 3D. CYP1A1 mRNA levels increased to a maximum at 8 h after exposure to indirubin and then declined, whereas CYP1A1 mRNA levels increased for up to 24 h after exposure to TCDD or B[a]P.

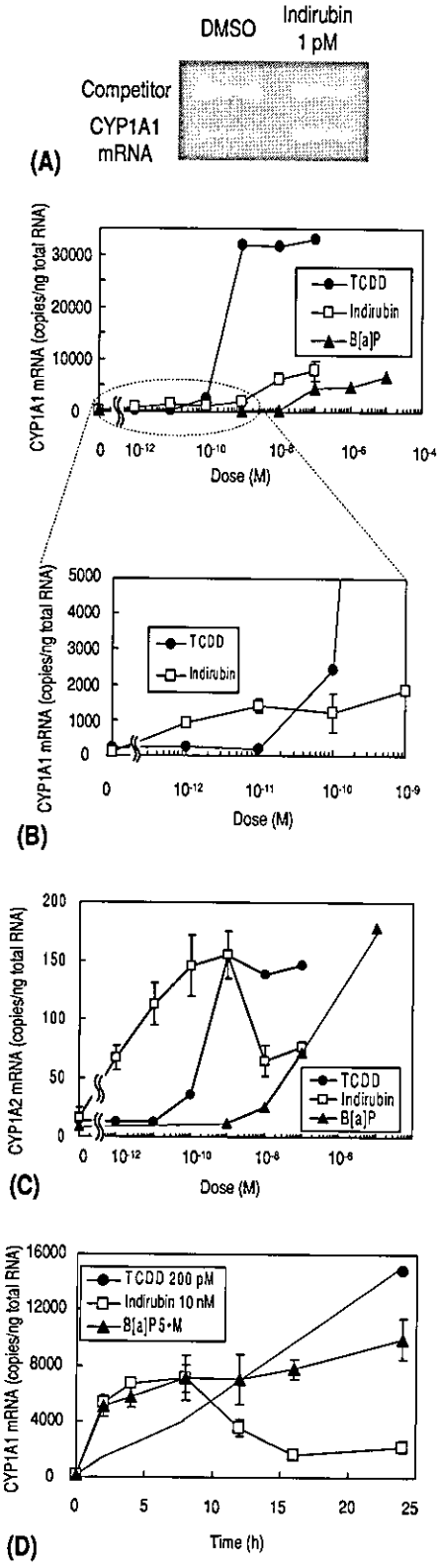

CYP2C, CYP2D6, CYP2E1, and CYP2A6 were confirmed to catalyze the production of indirubin from isatin *in vitro* (Gillam *et al.*, 2000), so we examined the mRNA expression levels of these enzymes. But we did not observe a significant induction of CYP2C, CYP2D6, CYP2E1, or CYP2A6 mRNA by indirubin (data not shown).

Metabolism of Indirubin by CYP1A1

To determine the metabolism of indirubin by CYP1A1, 100 nM of indirubin was mixed with recombinant human CYP1A1 and NADPH at 37°C for 3 h, and subsequently the AhR ligand activity was measured by assaying the AhR-responsive reporter gene activity of the yeast strain YCM3 (Adachi *et al.*, 2001). When indirubin was incubated with CYP1A1 and NADPH, the AhR ligand activity was dramatically decreased in the yeast assay in comparison with the control which did not contain CYP1A1 or NADPH (Fig. 4). These results indicate that indirubin is a substrate of the human CYP1A1 enzyme and that metabolism by CYP1A1 degrades indirubin's AhR binding activity.

Dissociation Constants of Indirubin, TCDD, and B[a]P for CYP1A1

Since we had not yet identified the indirubin metabolite, we could not determine the K_m and V_{max} values of this metabolic reaction. Alternatively, we measured the dissociation constants of indirubin, B[a]P, and TCDD for CYP1A1 to examine the interaction between the human CYP1A1 enzyme and these AhR ligands. To measure the dissociation constant, the degree of inhibition of 7-ethoxyresorufin O-deethylation (EROD) by each AhR ligand was determined. As shown in Figure 5, Lineweaver-Burk plots indicated that indirubin inhibited EROD activity by a mixed type inhibition as well as the typical CYP1A1 substrate B[a]P. The dissociation constant of indirubin and B[a]P represented by a Ki value was 2.9 and 7.4 nM, respectively. We also examined the inhibitory effect of TCDD, but no effect was observed at 775 nM of TCDD (data not shown).

FIG. 3. Effect of indirubin, TCDD, and B[a]P on CYP1A1 and CYP1A2 mRNA levels in HepG2 cells. (A) Induction of the CYP1A1 gene by 1 pM of indirubin. HepG2 cells were treated as described in Figure 2. CYP1A1 mRNA expression was quantified by competitive RT-PCR. (B) and (C) Dose-response curves of indirubin, TCDD and B[a]P for CYP1A1 (B) or CYP1A2 (C) mRNA induction. In Figure 3B, the lower panel shows part of the upper panel enlarged. Cells were treated with indirubin, TCDD, or B[a]P in the same conditions described in Figure 2. Error bars represent standard deviations obtained from three separate experiments. (D) Kinetics of CYP1A1 mRNA induction by indirubin, TCDD, and B[a]P. HepG2 cells were seeded into 10-cm dishes, and 24 h later a stock solution of indirubin, TCDD, or B[a]P in DMSO was added to the medium to yield a final concentration of 10 nM, 200 pM, or 5 µM, respectively. HepG2 cells were incubated from 0 to 24 h prior to total RNA isolation. Error bars represent standard deviations obtained from three separate experiments.

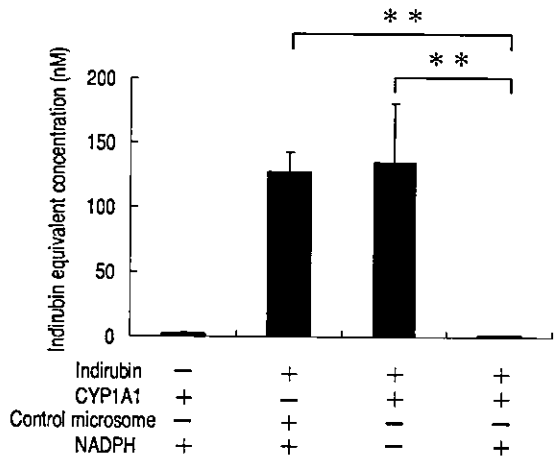

FIG. 4. Indirubin metabolism by human recombinant CYP1A1. Four types of reaction mixtures with or without indirubin, CYP1A1, control microsome, and NADPH were made as indicated at the bottom of the figure. Each reaction mixture (100 µl) was incubated at 37°C for 3 h. After the incubation, 1 µl of the mixture was subjected to a yeast assay and the equivalent concentration of indirubin was calculated from the dose-response curve of indirubin. The results obtained from three separate experiments were expressed as a histogram with standard deviations. **Significantly different from control ($p < 0.01$).

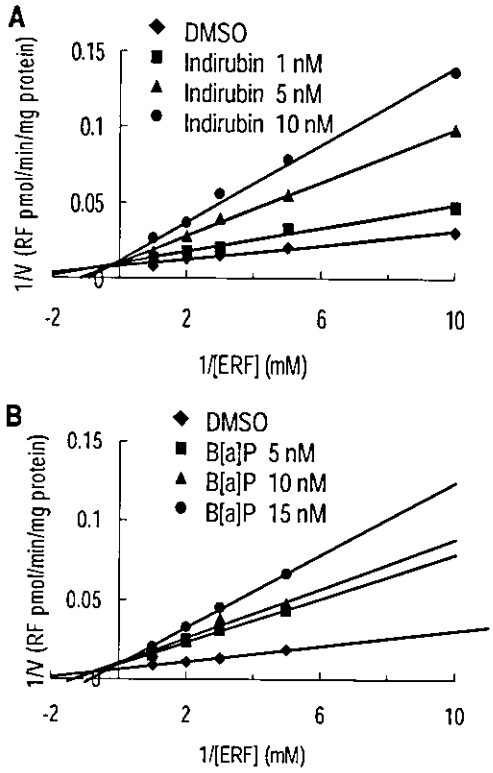

FIG. 5. Lineweaver-Burk plot for the inhibition of CYP1A1 enzyme activity by indirubin and B[a]P. The 7-ethoxyresorufin *O*-deethylation (EROD) activity of recombinant human CYP1A1 was inhibited by indirubin (A) and B[a]P (B). The Lineweaver-Burk plots suggest that indirubin and B[a]P are mixed-type inhibitors of EROD activity with a calculated *Ki* of 2.9 and 7.4 nM respectively.

DISCUSSION

The gene expression profile of TCDD in some cell lines and experimental animals has been reported (Frueh *et al.*, 2000; Hurst *et al.*, 2001; Kurachi *et al.*, 2002; Martinez *et al.*, 2002; Puga *et al.*, 2000; Zeytun *et al.*, 2002). In this study, we compared the gene expression profile of TCDD with that of the natural AhR ligand, indirubin. Genes whose expression was regulated by indirubin or TCDD were involved in xenobiotic metabolism (CYP1A1, CYP1A2, GSTP1), cytokine and cell signal transduction (IGFBP1, IGFBP10, IGF2, IL1R1, ILF2), steroid hormone and sex differentiation (TRIP15, CYP19A1, SOX9), cell cycle (CDKN1A, RBBP3, CDK1), cell adhesion (ITGB1, CDH2), transcriptional activation (EGR1, TCF12, BTF2p34), DNA replication and repair (TOP2A, TOP1, MSH2), and cholesterol and glucose transportation (NPC1, SLC2A2). The expression of CYP19A1, IGFBP1, and IGFBP10 mRNA was confirmed by real-time RT-PCR. There is a XRE-like sequence (5′-GCGTG-3′, −3139 ∼ −3135) in the promoter region of CYP19A1. Moreover, another AhR ligand, diindolylmethane (DIM), was reported to induce CYP19A1 expression in human adrenocortical carcinoma cells (Sanderson *et al.*, 2001). CYP19A1 is produced in hepatoma cells and responsible for the conversion of androgens to estrogens (Castagnetta *et al.*, 2003). These results suggest that CYP19A1 is an AhR-regulated gene. Further study is needed to elucidate whether the induction of CYP19A1 contributes to the estrogenic effect of TCDD. The mRNA expression of IGFBP1, 10 is a novel response to AhR ligands. IGFBP1 has an XRE sequence (5′-TNGCGTG-3′, − 87 ∼ −81) and an XRE-like sequence (−914 ∼ −910) in the promoter region. IGFBP10 also has three XRE sequences (−3116 ∼ −3110, −2360 ∼ −2354, −2233 ∼ −2227) and one XRE-like sequence (−392 ∼ −388). IGFBP1 is the smallest IGFBP and controls IGF-I's access to cell surface receptors. Excess levels of IGFBP1 may contribute to growth failure in intrauterine growth restriction and in pediatric chronic renal failure (Lee *et al.*, 1997). The binding affinity of IGFBP10 (CYR61/CCN1) for IGFs is two or three orders of magnitude less than that of IGFBP1 (Brigstock, 2003). IGFBP10 binds to cell surface integrins and induces intracellular signaling events that include kinase activation and gene transcription (Brigstock, 2003). IGFBP10 is estrogen-inducible and overexpressed in steroid-dependent breast tumors and promotes breast cancer. It also plays an essential role in placental angiogenesis during embryogenesis. These mRNA inductions *in vitro* require further study in animal models *in vivo*. AhR was implicated in cell cycle arrest at G1 (Ma and Whitlock, 1996; Weiss *et al.*, 1996) through the down-regulation of cyclins and cyclin-dependent kinases, and/or by induction of cyclin-dependent kinase inhibitors such as p21

(CDKN1A) (Cover *et al.*, 1999; Kolluri *et al.*, 1999; Rininger *et al.*, 1997; Yoon *et al.*, 2002). In our microarray analysis, CDKN1A was up-regulated and RBBP3 (E2F1) and CDK1 (Cdc2) were down-regulated. RBBP3 is inactive when bound to retinoblastoma (RB) protein (Nevins, 2001). When RB is phosphorylated by CDK4, RBBP3 uncouples from RB and works as a transcription factor to move the cell cycle from G1 to S. CDK1 is a member of the Ser/Thr protein kinase family and a catalytic subunit of the highly conserved protein kinase complex known as M-phase promoting factor (MPF), which is essential for the G2/M transition in the eukaryotic cell cycle (Doree and Hunt, 2002). So, indirubin and TCDD-mediated activation of AhR may produce an arrest in G1 and G2 of the cell cycle via the transcriptional regulation of CDKN1A, RBBP3, and CDK1. Interestingly, indirubin also inhibits several CDKs and other kinases directly (Hoessel *et al.*, 1999). Thus, indirubin may control the cell cycle via AhR-dependent and independent pathways. As shown in Table 2, the pattern of gene expression was almost the same between indirubin and TCDD. Technical developments that offer increased sensitivity when examining large numbers of genes for a given organism should make it possible to evaluate changes in RNA expression comprehensively and identify indirubin or TCDD-specific genes sometime soon.

We observed that CYP1A1 mRNA levels transiently increased to 2550 copies/ng total RNA at 8 h and dropped to 100 copies/ng total RNA at 32 h after the change of medium without adding any AhR ligands in HepG2 cells. It was also reported that CYP1A1 mRNA expression was transiently induced by FBS in HepG2 cells (Guigal *et al.*, 2001). We speculate that indirubin in FBS primarily contributes to the induction. This is because (1) indirubin accounted for half of the total AhR activity of FBS in our previous study (Adachi *et al.*, 2001), (2) both indirubin and FBS induce CYP1A1 mRNA expression transiently, and (3) the concentration of indirubin in FBS is sufficient (0.07 nM) to induce CYP1A1 mRNA expression.

The lowest observed effective concentration (LOEC) for CYP1A1 mRNA induction by indirubin and TCDD was 1 pM and 100 pM, respectively. The LOEC for CYP1A2 mRNA induction was the same as for CYP1A1 mRNA induction. As far as we know, no other AhR ligand has been reported to induce CYP1A mRNA expression at 1 pM in human cells. However, the maximum induction level of CYP1A1 differed between TCDD and indirubin, whereas that of CYP1A2 was the same for the two chemicals. This differential induction of CYP1A1 vs. CYP1A2 by TCDD compared to indirubin may due to differences in the location and number of XRE, transcription factors other than AhR, mRNA stability and AhR degradation by a ubiquitination-dependent mechanism. Moreover the dominant induction of CYP1A1 compared to CYP1A2 is important information with regard to the metabolism of AhR ligands. The data on the potency of indirubin and TCDD obtained from our study using human cells agrees with that obtained in the yeast AhR signalling assay (Adachi *et al.*, 2001). We found that indirubin is able to induce CYP1A1 and CYP1A2 mRNA expression in human cells at the physiological concentration. Therefore, it seems reasonable to suppose that indirubin is an endogenous AhR ligand activating AhR-mediated signaling mechanisms in human cells.

As shown in the time-course experiment (Fig. 3D), 10 nM of indirubin induced CYP1A1 mRNA expression transiently, whereas 200 pM of TCDD induced expression throughout 24 h. It was reported that 1 nM of TCDD also induced CYP1A1 enzyme activity (as detected with the EROD assay) steadily over a 24 h period in HepG2 cells (Chen *et al.*, 1995). In contrast to TCDD, another putative endogenous AhR ligand, lipoxin A4, was reported to induce CYP1A1 mRNA expression transiently (maximum level at 8 h) in a similar manner to indirubin (Schaldach *et al.*, 1999). A transient CYP1A1 mRNA induction is consistent with the finding data that CYP1A1 mRNA was rapidly degraded in HepG2 cells ($t_{0.5}$ = 2.4 h) (Lekas *et al.*, 2000). Thus we hypothesized that the transient CYP1A1 mRNA induction was due to the metabolism of indirubin by the induced enzyme (CYP1A1). The indirubin metabolism experiment (Fig. 4) clearly supported this hypothesis. We measured the dissociation constant between indirubin and CYP1A1 to supply this metabolic response with a quantitative underpinning. The dissociation constant of indirubin and B[a]P represented by Ki was 2.9 and 7.4 nM, respectively. K_i values of other AhR ligands, lipoxin A4 and resveratrol, were reported to be 1100 and 1200 nM respectively under the similar experimental conditions (Chang *et al.*, 2001; Schaldach *et al.*, 1999). To our knowledge, the dissociation constant of indirubin-CYP1A1 is the lowest value reported among CYP1A1 substrates. TCDD did not inhibit the EROD activity in our experiment using human CYP1A1 and it was reported that TCDD competitively inhibited the EROD activity (K_i value, 200 nM) using rat hepatic microsomes (Petrulis and Bunce, 1999). Our results do not directly show but strongly suggest, that indirubin will efficiently bind the substrate-binding site of CYP1A1 and be rapidly metabolized, whereas TCDD will not be metabolized by CYP1A1 effectively. In MCF-7 human breast cancer cells, indirubin induced CYP1A1 and 1B1 expression transiently and the potency of indirubin increased when cells were treated with the CYP inhibitor, ellipticine (Spink *et al.*, 2003). The K_i of a well known CYP1A1 substrate, B[a]P, was as low as that of indirubin. However, the long-term induction of CYP1A1 mRNA expression by B[a]P (Fig. 3D) was observed. One of its metabolites benzo[a]pyrene-7,8-dione (BPQ) may contribute to this induction, because it was found to be a potent and rapid inducer of CYP1A1 mRNA, with an EC_{50} value identical to that of the parent B[a]P in HepG2 cells (Burczynski and Penning, 2000).

Inducing the expression of drug-metabolizing enzymes is a well known function of AhR. But AhR also plays roles in cell-cycle regulation (Cover *et al.*, 1999; Kolluri *et al.*, 1999; Ma and Whitlock, 1996; Rininger *et al.*, 1997; Weiss *et al.*, 1996; Yoon *et al.*, 2002), cell differentiation (Phillips *et al.*, 1995), the development of organs (Fernandez-Salguero *et al.*, 1995, 1996;

Schmidt *et al.*, 1996), and the modification of hormone signalling by cross-talk with hormone receptors (Ohtake *et al.*, 2003). Which is the primary role of AhR? One view is that the primary role of AhR is the latter and such physiological roles are triggered by a "true" AhR ligand like hormones or vitamins. CYP1A1 may have been developed to control the level of the ligand in cells. Another view is that the primary role of AhR is just to detoxify toxic AhR ligands. The majority of natural AhR ligands identified to date are dietary or related to dietary plant products (Denison *et al.*, 2002). Among these ligands, indirubin was reported to inhibit the activity of many kinases, such as GSK-3β, CDKs, extracellular-signal-regulated kinase 2 (Erk2), casein kinase 1, and c-Src tyrosine kinase (Hoessel *et al.*, 1999). An indirubin derivative was also reported to inhibit CDK2 via direct interaction with the kinase's ATP binding site (Hoessel *et al.*, 1999). Therefore, it may be reasonable to conclude that if indirubin is not be metabolized, it may accumulate in some organs because of its hydrophobic nature and cause toxicity via direct inhibition of kinases. The other functions like cell-cycle arrest via AhR may have developed to transiently stop the cell cycle when the drug-metabolizing enzymes are running at full capacity.

Since, as far as we know, indirubin is the most potent AhR ligand, and shows strongest affinity for CYP1A1, it is reasonable to speculate that a natural AhR ligand like indirubin, rather than environmental AhR ligands such as dioxins and PAHs, promoted the evolution of the AhR-CYP1A1 system.

ACKNOWLEDGMENTS

We wish to thank Dr. Charles A. Miller III (Environmental Health Sciences Department and Tulane-Xavier Center for Bioenvironmental Research, Tulane University, New Orleans, LA) for providing the yeast strain YCM3 and for helpful suggestions and Dr. Ken-ichi Saeki (Faculty of Pharmaceutical Sciences, Nagoya City University) for providing indirubin. This work was supported in part by the Japanese Ministry of the Environment, the Japanese Ministry of Health, Labour and Welfare and Grants-in-aid for Scientific Research 13027245 and 12055101 from the Japanese Ministry of Education, Science, Sports and Culture, and New England and Industrial Technology Development Organization (NEDO). J.A. was supported in part by a J.S.P.S. Research Fellowship for Young Scientists.

REFERENCES

Adachi, J., Mori, Y., Matsui, S., Takigami, H., Fujino, J., Kitagawa, H., Miller, C. A. 3rd, Kato, T., Saeki, K., and Matsuda, T. (2001). Indirubin and indigo are potent aryl hydrocarbon receptor ligands present in human urine. *J. Biol. Chem.* **276,** 31475–31478.

Brigstock, D. R. (2003). The CCN family: A new stimulus package. *J. Endocrinol.* **178,** 169–175.

Burczynski, M. E., and Penning, T. M. (2000). Genotoxic polycyclic aromatic hydrocarbon ortho-quinones generated by aldo-keto reductases induce CYP1A1 via nuclear translocation of the aryl hydrocarbon receptor. *Cancer Res.* **60,** 908–915.

Castagnetta, L. A., Agostara, B., Montalto, G., Polito, L., Campisi, I., Saetta, A., Itoh, T., Yu, B., Chen, S., and Carruba G. (2003). Local estrogen formation by nontumoral, cirrhotic, and malignant human liver tissues and cells. *Cancer Res.* **63,** 5041–5045.

Chang, T. K., Chen, J., and Lee, W. B. (2001). Differential inhibition and inactivation of human CYP1 enzymes by trans-resveratrol: Evidence for mechanism-based inactivation of CYP1A2. *J. Pharmacol. Exp. Ther.* **299,** 874–882.

Chen, Y. H., Riby, J., Srivastava, P., Bartholomew, J., Denison, M., and Bjeldanes, L. (1995). Regulation of CYP1A1 by indolo[3,2-b]carbazole in murine hepatoma cells. *J. Biol. Chem.* **270,** 22548–22555.

Cover, C. M., Hsieh, S. J., Cram, E. J., Hong, C., Riby, J. E., Bjeldanes, L. F., and Firestone, G. L. (1999). Indole-3-carbinol and tamoxifen cooperate to arrest the cell cycle of MCF-7 human breast cancer cells. *Cancer Res.* **273,** 1244–1251.

Denison, M. S., Pandini, A., Nagy, S. R., Baldwin, E. P., and Bonati, L. (2002). Ligand binding and activation of the Ah receptor. *Chem. Biol. Interact.* **141,** 3–24.

Doree, M., and Hunt, T. (2002). From Cdc2 to Cdk1: When did the cell cycle kinase join its cyclin partner? *J. Cell Sci.* **15,** 2461–2464.

Fernandez-Salguero, P. M., Hilbert, D. M., Rudikoff, S., Ward, J. M., and Gonzalez, F. J. (1996). Aryl-hydrocarbon receptor-deficient mice are resistant to 2,3,7,8-tetrachlorodibenzo-*p*-dioxin-induced toxicity. *Toxicol. Appl. Pharmacol.* **140,** 173–179.

Fernandez-Salguero, P. M., Pineau, T., Hilbert, D. M., McPhail, T., Lee, S. S., Kimura, S., Nebert, D. W., Rudikoff, S., Ward, J. M., and Gonzalez, F. J. (1995). Immune system impairment and hepatic fibrosis in mice lacking the dioxin-binding Ah receptor. *Science* **5,** 722–726.

Frueh, F. W., Hayashibara, K. C., Brown, P. O., and Whitlock Jr., J. P. (2000). Use of cDNA microarrays to analyze dioxin-induced changes in human liver gene expression. *Toxicol. Lett.* **45,** 189–203.

Gaido, K. W., and Maness, S. C. (1994). Regulation of gene expression and acceleration of differentiation in human keratinocytes by 2,3,7,8-tetrachlorodibenzo-*p*-dioxin. *Toxicol. Appl. Pharmacol.* **127,** 199–208.

Gillam, E. M. J., Notley, L. M., Cai, H., De Voss, J. J., and Guengerich, F. P. (2000). Oxidation of indole by cytochrome P450 enzymes. *Biochemistry* **39,** 13817–13824.

Guigal, N., Seree, E., Nguyen, Q. B., Charvet, B., Desobry, A., and Barra, Y. (2001). Serum induces a transcriptional activation of CYP1A1 gene in HepG2 independently of the AhR pathway. *Life Sci.* **68,** 2141–2150.

Hoessel, R., Leclerc, S., Endicott, J. A., Nobel, M. E. M., Lawrie, A., Tunnah, P., Leost, M., Damiens, E., Marie, D., Marko, D., Niederberger, E., Tang, W., Eisenbrand, G., and Meijer, L. (1999). Indirubin, the active constituent of a Chinese antileukaemia medicine, inhibits cyclin-dependent kinases. *Nat. Cell Biol.* **1,** 60–67.

Hurst, C. H., Abbott, B., Schmid, J. E., and Birnbaum, L. S. (2001). 2,3,7,8-Tetrachlorodibenzo-*p*-dioxin (TCDD) disrupts early morphogenetic events that form the lower reproductive tract in female rat fetuses. *Toxicol. Sci.* **508,** 87–98.

Jeon, M. S., and Esser, C. (2000). The murine IL-2 promoter contains distal regulatory elements responsive to the Ah receptor, a member of the evolutionarily conserved bHLH-PAS transcription factor family. *J. Immunol.* **165,** 6975–6983.

Kolluri, S. K., Weiss, C., Koff, A., and Gottlicher, M. (1999). p27(Kip1) induction and inhibition of proliferation by the intracellular Ah receptor in developing thymus and hepatoma cells. *Genes Dev.* **13,** 1742–1753.

Kunikata, T., Tatefuji, T., Aga, H., Iwaki, K., Ikeda, M., and Kurimoto, M. (2000). Indirubin inhibits inflammatory reactions in delayed-type hypersensitivity. *Eur. J. Pharmacol.* **410,** 93–100.

Kurachi, M., Hashimoto, S., Obata, A., Nagai, S., Nagahata, T., Inadera, H., Sone, H., Tohyama, C., Kaneko, S., Kobayashi, K., and Matsushima, K.

(2002). Identification of 2,3,7,8-tetrachlorodibenzo-*p*-dioxin-responsive genes in mouse liver by serial analysis of gene expression. *Biochem. Biophys. Res. Commun.* **65,** 368–377.

Lee, P. D., Giudice, L. C., Conover, C. A., and Powell, D. R. (1997) Insulin-like growth factor binding protein-1: Recent findings and new directions. *Proc. Soc. Exp. Biol. Med.* **216,** 319–357.

Lekas, P., Tin, K. L., Lee, C., and Prokipcak, R. D. (2000). The human cytochrome P450 1A1 mRNA is rapidly degraded in HepG2 cells. *Arch. Biochem. Biophys.* **384,** 311–318.

Lu, Y., Wang, X., and Safe, S. (1994). Interaction of 2,3,7,8-tetrachlorodibenzo-*p*-dioxin and retinoic acid in MCF-7 human breast cancer cells. *Toxicol. Appl. Pharmacol.* **127,** 1–8.

Lucier, G. W., Portier, C. J., and Gallo, M. A. (1993). Receptor mechanisms and dose-response models for the effects of dioxins. *Environ. Health Perspect.* **22,** 36–44.

Ma, Q., and Whitlock Jr., J. P. (1996). The aromatic hydrocarbon receptor modulates the Hepa 1c1c7 cell cycle and differentiated state independently of dioxin. *Mol. Cell. Biol.* **271,** 2144–2150.

Martinez, J. M., Afshari, C. A., Bushel, P. R., Masuda, A., Takahashi, T., and Walker, N. J. (2002). Differential toxicogenomic responses to 2,3,7,8-tetrachlorodibenzo-*p*-dioxin in malignant and nonmalignant human airway epithelial cells. *Toxicol. Sci.* **141,** 409–423.

Miller, C. A. 3rd. (1999). A human aryl hydrocarbon receptor signaling pathway constructed in yeast displays additive responses to ligand mixtures. *Tox. Appl. Pharmacol.* **160,** 297–303.

Mimura, J., Yamashita, K., Nakamura, K., Morita, M., Takagi, T. N., Nakao, K., Ema, M., Sogawa, K., Yasuda, M., Katsuki, M., and Fujii-Kuriyama, Y. (1997). Loss of teratogenic response to 2,3,7,8-tetrachlorodibenzo-*p*–dioxin (TCDD) in mice lacking the Ah (dioxin) receptor. *Genes to Cells* **2,** 645–654.

Moore, M., Narasimhan, T. R., Steinberg, M. A., Wang, X., and Safe, S. (1993). Potentiation of CYP1A1 gene expression in MCF-7 human breast cancer cells cotreated with 2,3,7,8-tetrachlorodibenzo-*p*-dioxin and 12-*O*-tetradecanoylphorbol-13-acetate. *Arch. Biochem. Biophys.* **305,** 483–488.

Nebert, D. W., Roe, A. L., Dieter, M. Z., Solis, W. A., Yang, Y., and Dalton, T. P. (2000). Role of the aromatic hydrocarbon receptor and [Ah] gene battery in the oxidative stress response, cell cycle control, and apoptosis. *Biochem. Pharmacol.* **59,** 65–85.

Nevins, J. R. (2001). The Rb/E2F pathway and cancer. *Hum. Mol. Genet.* **10,** 699–703.

Ohtake, F., Takeyama, K., Matsumoto, T., Kitagawa, H., Yamamoto, Y., Nohara, K., Tohyama, C., Krust, A., Mimura, J., Chambon, P., Yanagisawa, J., Fujii-Kuriyama, Y., and Kato, S. (2003). Modulation of oestrogen receptor signalling by association with the activated dioxin receptor. *Nature* **423,** 545–550.

Petrulis, J. R., and Bunce, N. J. (1999). Competitive inhibition by inducer as a confounding factor in the use of the ethoxyresorufin-*O*-deethylase (EROD) assay to estimate exposure to dioxin-like compounds. *Toxicol. Lett.* **105,** 251–260.

Phillips, M., Enan, E., Liu, P. C., and Matsumura, F. (1995). Inhibition of 3T3-L1 adipose differentiation by 2,3,7,8-tetrachlorodibenzo-*p*-dioxin. *J. Cell Sci.* **108,** 395–402.

Pohjanvirta, R., and Tuomisto, J. (1994). Short-term toxicity of 2,3,7,8-tetrachlorodibenzo-*p*-dioxin in laboratory animals: Effects, mechanisms, and animal models. *Pharmacol. Rev.* **46,** 483–549.

Puga, A., Nebert, D. W., and Carrier, F. (1992). Dioxin induces expression of c-fos and c-jun proto-oncogenes and a large increase in transcription factor AP-1. *DNA Cell Biol.* **11,** 269–281.

Puga, A., Hoffer, A., Zhou, S., Bohm, J. M., Leikauf, G. D., and Shertzer, H. G. (1997). Sustained increase in intracellular free calcium and activation of cyclooxygenase-2 expression in mouse hepatoma cells treated with dioxin. *Biochem. Pharmacol.* **54,** 1287–1296.

Puga, A., Maier, A., and Medvedovic, M. (2000). The transcriptional signature of dioxin in human hepatoma HepG2 cells. *Biochem. Pharmacol.* **60,** 1129–1142.

Rannug, U., Bramstedt, H., and Nilsson, U. (1992). The presence of genotoxic and bioactive components in indigo dyed fabrics—a possible health risk? *Mutat. Res.* **282,** 219–25.

Rininger, J. A., Stoffregen, D. A., Babish, J. G. (1997). Murine hepatic p53, RB, and CDK inhibitory protein expression following acute 2,3,7,8-tetrachlorodibenzo-*p*-dioxin (TCDD) exposure. *Chemosphere* **51,** 1557–1568.

Sanderson, J. T., Slobbe, L., Lansbergen, G. W., Safe, S., and van den Berg, M. (2001). 2,3,7,8-Tetrachlorodibenzo-p-dioxin and diindolylmethanes differentially induce cytochrome P450 1A1, 1B1, and 19 in H295R human adrenocortical carcinoma cells. *Toxicol. Sci.* **61,** 40–48.

Schaldach, C. M., Riby, J., and Bjeldanes, L. F. (1999). Lipoxin A4: A new class of ligand for the Ah receptor. *Biochemistry* **38,** 7594–7600.

Schmidt, J. V., Su, G. H., Reddy, J. K., Simon, M. C., and Bradfield, C. A. (1996). Characterization of a murine Ahr null allele: Involvement of the Ah receptor in hepatic growth and development. *Proc. Natl. Acad. Sci. U.S.A.* **93,** 6731–6736.

Spink, B. C., Hussain, M. M., Katz, B. H., Eisele, L., and Spink, D. C. (2003). Transient induction of cytochromes P450 1A1 and 1B1 in MCF-7 human breast cancer cells by indirubin. *Biochem. Pharmacol.* **66,** 2313–2321.

Vogel, C., and Abel, J. (1995). Effect of 2,3,7,8-tetrachlorodibenzo-*p*-dioxin on growth factor expression in the human breast cancer cell line MCF-7. *Arch. Toxicol.* **69,** 259–265.

Weiss, C., Kolluri, S. K., Kiefer, F., and Gottlicher, M. (1996). Complementation of Ah receptor deficiency in hepatoma cells: Negative feedback regulation and cell cycle control by the Ah receptor. *Exp. Cell. Res.* **226,** 154–163.

Wolfle, D., Marotzki, S., Dartsch, D., Schafer, W., and Marquardt, H. (2000). Induction of cyclooxygenase expression and enhancement of malignant cell transformation by 2,3,7,8-tetrachlorodibenzo-*p*-dioxin. *Carcinogenesis* **21,** 15–21.

Yoon, B. I., Hirabayashi, Y., Kawasaki, Y., Kodama, Y., Kaneko, T., Kanno, J., Kim, D. Y., Fujii-Kuriyama, Y., and Inoue, T. (2002). Aryl hydrocarbon receptor mediates benzene-induced hematotoxicity. *Toxicol. Sci.* **70,** 150–156.

Zeytun, A., McKallip, R. J., Fisher, M., Camacho, I., Nagarkatti, M., and Nagarkatti, P. S. (2002). Analysis of 2,3,7,8-tetrachlorodibenzo-*p*-dioxin-induced gene expression profile *in vivo* using pathway-specific cDNA arrays. *Toxicology* **23,** 241–260.

Accelerated Publication

THE JOURNAL OF BIOLOGICAL CHEMISTRY
Vol. 276, No. 34, Issue of August 24, pp. 31475–31478, 2001

Indirubin and Indigo Are Potent Aryl Hydrocarbon Receptor Ligands Present in Human Urine*

Received for publication, May 10, 2001, and in revised form, June 1, 2001
Published, JBC Papers in Press, June 25, 2001,
DOI 10.1074/jbc.C100238200

Jun Adachi‡, Yoshitomo Mori‡, Saburo Matsui‡, Hidetaka Takigami§, Junko Fujino§, Hiroko Kitagawa§, Charles A. Miller III¶‖, Takaaki Kato, Kenichi Saeki**, and Tomonari Matsuda§‡‡**

*From the ‡Department of Environmental Engineering, Kyoto University, Sakyo-Ku, Yoshida-Honmachi, Kyoto 606-8501, Japan, §Research Center for Environmental Quality Control, Kyoto University, 1-2 Yumihama, Otsu 520-0811, Japan, ¶Department of Environmental Health Sciences and Tulane-Xavier Center for Bioenvironmental Research, Tulane University School of Public Health and Tropical Medicine, New Orleans, Louisiana 70112, and **Faculty of Pharmaceutical Sciences, Nagoya City University, Tanabedori, Mizuho-ku, Nagoya 467-8603, Japan*

Aryl hydrocarbon receptor (AhR) is a ligand-activated transcription factor that regulates genes involved in xenobiotic metabolism, cellular proliferation, and differentiation. Numerous xenobiotic and biological compounds are known to interact with AhR, but it remains an orphan receptor, because its physiological ligand is unknown. We identified AhR ligands in human urine using a yeast AhR signaling assay and then characterized their properties. Two ligands, indirubin and indigo, were both present at average concentrations of ~0.2 nM in the urine of normal donors. Indirubin was also detected in fetal bovine serum and contributed half of the total AhR ligand activity. The activities of indirubin and indigo were comparable with or more potent than that of the archetypal ligand, 2,3,7,8-tetrachlorodibenzo-*p*-dioxin, in yeast AhR activation assays. We suggest that the endogenous levels and potencies of indirubin and indigo are such that they activate AhR-mediated signaling mechanisms *in vivo*.

AhR,[1] also called the dioxin receptor, is a ligand-activated transcription factor that is present in most cell and tissue types of the body (1). AhR-mediated signaling is required for potent xenobiotic ligands such as TCDD and polychlorinated biphenyls to produce toxic responses (2, 3). Toxic effects that are linked to xenobiotic AhR ligand exposures in animals include cancers, reproductive impairment, endometriosis, birth defects, and immunological impairment (4–6). The toxic potential of xenobiotic AhR ligands is currently a major concern for regulatory agencies that are responsible for protecting public and environmental health.

Although numerous xenobiotic ligands for AhR have been identified, the AhR is considered to be an orphan receptor, because its physiological ligand(s) and its function are not known. Tryptophan and other indole-containing compounds (7–9), bilirubin (10), 7-ketocholesterol (11), lipoxin A4 (12), flavones, and related compounds (13) interact with AhR to produce activation or inhibition of signal transduction. In general, the low levels, lack of potency, and restricted distribution of these compounds make them unlikely candidates as major regulators of AhR signaling in most tissue types. We reasoned that human urine might be a good place to search for endogenous AhR ligands, and we developed a methodology to detect and isolate such compounds.

EXPERIMENTAL PROCEDURES

Materials—Blue rayon was kindly provided by Dr. Hayatsu (Okayama University, Okayama City, Japan). General chemicals, essentially analytical grade, were purchased from Wako (Kyoto, Japan). TCDD was purchased from CIL (Andover, MA, USA). Indigo and β-glucuronidase were purchased from Sigma. Indirubin was synthesized as described in Hoessel *et al.* (14). Indigo and indirubin were further purified by HPLC before use.

Yeast Assay for AhR Ligand Activity—The assay procedure was essentially as described by Miller (15). The yeast strain YCM3 was grown overnight at 30 °C in synthetic glucose medium lacking tryptophan. Test chemicals (dissolved in Me_2SO), 5 μl of the overnight culture, and 200 μl of synthetic medium containing 2% galactose were mixed in a 96-well microplate with subsequent incubation for 18 h at 30 °C. The cell densities were determined by reading the absorbance at 595 nm. 10 μl of each cell suspension was added to 140 μl of Z-buffer (60 mM Na_2HPO_4, 40 mM NaH_2PO_4, 1 mM $MgCl_2$, 10 mM KCl, 2 mM dithiothreitol, and 0.2% sarcosyl, adjusted to pH 7), and the reaction was started by adding 50 μl of *o*-nitrophenol-β-D-galactopyranoside (4 mg/ml solution in Z-buffer) with subsequent incubation for 60 min at 37 °C. Absorbances of the β-galactosidase assays were read at 405 nm. β-Galactosidase activity (referred to as lacZ units) was calculated by the following formula: absorbance at 405 nm × 1000/(absorbance at 595 nm × ml of cell suspension added × min of reaction time). TCDD equivalent concentration was calculated from the dose-response curve of TCDD.

Isolation of AhR Ligands from Human Urine—Human urine was collected from healthy male volunteers. The urine (5 liters per batch) was treated with H_2SO_4 (final concentration 0.5 N) at 60 °C for 1 h followed by neutralization with NaOH. Blue rayon (5 g) was added to the 5 liters of urine and stirred for 1 h at room temperature. The blue rayon was removed from urine, washed with water, dried, and extracted twice with 200 ml of methanol:ammonia (50:1, v/v). The extract was evaporated to dryness and then dissolved in 2 ml of Me_2SO. The urine sample concentrated by absorption to blue rayon was applied to a Sephadex LH-20 column (5.0 × 20.0 cm; Amersham Pharmacia Biotech) and eluted with methanol (1.5 ml/min). The fractions at elution volume of 615–720 ml were collected and evaporated to dryness. The residue was dissolved in a small volume of Me_2SO and applied to a

* This work was supported in part by Grants-in-aid for Scientific Research 11750490, 12055101, and 12771444 from the Japanese Ministry of Education, Science, Sports and Culture, by the Fundamental Research Fund for the Environmental Future ("Assessment and Control of Risks to Progeny from Exposure to Complex Chemicals in the Environment") from the Japanese Ministry of the Environment, and by National Institutes of Health Grant ES09055. The costs of publication of this article were defrayed in part by the payment of page charges. This article must therefore be hereby marked "*advertisement*" in accordance with 18 U.S.C. Section 1734 solely to indicate this fact.

‖ To whom requests for the yeast strain should be addressed. Tel.: 504-585-6942; Fax: 504-585-6942; E-mail: rellim@tulane.edu.

‡‡ To whom correspondence should be addressed. Tel.: 81-77-527-6224; Fax: 81-77-524-9869; E-mail: matsuda@biwa.eqc.kyoto-u.ac.jp.

[1] The abbreviations used are: AhR, Aryl hydrocarbon receptor; TCDD, 2,3,7,8-tetrachlorodibenzo-*p*-dioxin; ARNT, aryl hydrocarbon receptor nuclear translocator; FBS, fetal bovine serum; CDK, cyclin-dependent kinase; HPLC, high pressure liquid chromatography.

reversed-phase column (μ BONDASPHERE 15-μ C_{18}, ϕ19 × 150 mm; Waters Corp., Milford, MA), eluted at a flow rate of 5 ml/min with 80% methanol/water (v/v) for purification of the AhR ligands.

Quantification of Indirubin and Indigo in Human Urine and FBS—Urine samples were collected from healthy volunteers and were treated immediately after excretion as follows. Urine was passed through a glass filter, and 100 ml of the filtrate was then passed through a Sep-Pak C_{18} cartridge (Waters). The cartridge was washed with 20 ml of water and 10 ml of 50% (v/v) methanol/water. Indirubin and indigo were eluted with 5 ml of Me_2SO followed by the evaporation to dryness by centrifugal concentrator. The residue was dissolved in 100 μl of Me_2SO and injected to an analytical reversed-phase column (symmetry C_{18}/5 μm, ϕ4.6 × 250 mm; Waters), eluted with 70% (v/v) methanol/water at a flow rate of 1 ml/min. The fractions collected every min were evaporated to dryness followed by dissolving in 50 μl of Me_2SO. The yeast assay was carried out on the samples to estimate the AhR ligand activity of the fractions corresponding to the retention time of indigo and indirubin. The recovery of the standard indigo and indirubin using this method was over 95%. Dilutions of indirubin and indigo standards were also tested at the same time to generate the standard curves. FBS was purchased from JRH Biosciences (Lenexa, KS). Indirubin and indigo in FBS were measured under the same method except for the HPLC condition. We used an analytical reversed-phase column (Wakosil-II-5C_{18}, ϕ4.6 × 250 mm; Wako, Japan), eluted with the following gradient system of methanol in water: 0–20 min, linear gradient of 65–100%; 20–40 min, 100% at a flow rate of 0.5 ml/min.

RESULTS AND DISCUSSIONS

AhR ligand activity in human urine was assessed with a reporter gene assay using the *Saccharomyces cerevisiae* strain YCM3, in which the human AhR and ARNT genes were co-expressed. Ligand-dependent activation of AhR leads to formation of a AhR/ARNT heterodimer that, in turn, stimulates transcriptional activation of a lacZ reporter plasmid in this assay (Fig. 1*A*). Thus, AhR ligand activity in urine fractions can be detected and quantified by measuring β-galactosidase activity.

Human urine collected from healthy volunteers was concentrated with the planar-compound specific absorbent blue rayon (16). The yeast assay revealed that human urine contains AhR ligand(s), and their activity was observed even in unconcentrated levels (concentration factor = 1) (Fig. 1*B*). Treatment of urine with β-glucuronidase significantly increased the AhR ligand activity (10-fold), and treatment with H_2SO_4 dramatically raised the activity (1,000-fold). These results suggested the presence of the glucuronide and sulfate conjugates of the ligands. It is also possible that ligand precursors were present in urine and that acid treatment process caused the formation of the ligands.

Human urine treated with H_2SO_4 was concentrated by blue rayon and subjected to fractionation by HPLC. Each fraction was assayed for AhR ligand activity by the yeast assay. Fig. 1*C* shows the HPLC elution profile, along with absorbance (540 nm) and AhR ligand activity, of each fraction. Two major active fractions with retention times of 9–11 and 17–22 min were observed. The AhR ligand activity in these two fractions accounted for 5 and 90%, respectively, of the total activity. The two absorbance peaks (540 nm) corresponding to the active fractions were designated as B1 (blue compound 1) and R1 (red compound 1), respectively (Fig. 1*D*).

To investigate whether these compounds were present in untreated human urine, 5 liters of untreated urine was concentrated using blue rayon and analyzed by HPLC with a photodiode array detector. The UV-visible spectral absorption patterns showed clear peaks that corresponded to those of B1 and R1 (data not shown). Moreover, 100 ml of untreated fresh urine was concentrated using a Sep-Pak C_{18} cartridge instead of blue rayon, injected to HPLC, fractionated every 1 min, and activity was followed using the yeast AhR assay. The major AhR ligand activity was observed in the fractions that eluted at the same time as B1 and R1 (Fig. 1*E*). These results indicated that B1

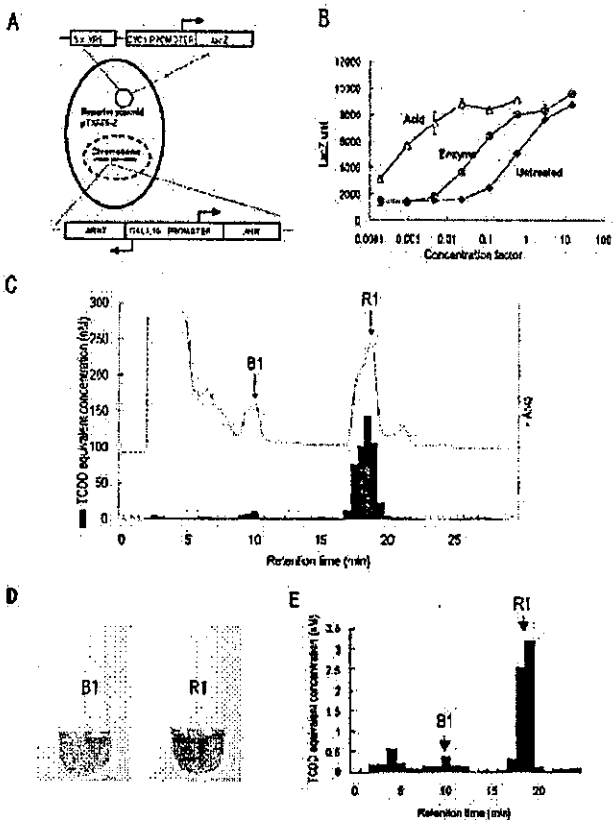

FIG. 1. **Presence of AhR ligands in human urine.** *A*, the features of the recombinant yeast strain YCM3. The human AhR and ARNT genes are integrated into chromosome III. AhR and ARNT are expressed from the galactose-regulated GAL 1,10 promoter. Transcriptional activation mediated by the AhR/ARNT heterodimer is assessed by β-galactosidase activity. Expression of the lacZ reporter plasmid, pTXRE5-Z, is directed by AhR·Arnt complex binding to five response elements in the promoter region. *B*, AhR ligand activity of human urine. Urine was concentrated by blue rayon directly (*closed diamonds*) or treated with 1000 units/ml of β-glucuronidase (*open circles*) for 24 h at 37 °C or 0.5 N H_2SO_4 (*open triangles*) for 1 h at 60 °C. Each datum is the mean ± S.D. of duplicate experiments. *C*, HPLC elution profile of AhR ligand activity in acid-treated urine resolved using an analytical Symmetry C_{18} column (ϕ4.6 × 250 mm; Waters) by elution with 70% (v/v) methanol/water, at a flow rate of 1 ml/min. The absorbance (*upper line*) was monitored at 540 nm. The AhR ligand activity of each 0.5-min fraction (*bars*) was tested by the yeast assay. TCDD equivalent concentration was calculated from the LacZ units of each fractions and the dose-response curve of TCDD. *D*, the *color images* of the extracts dissolved in Me_2SO (*left*, B1; *right*, R1). The UV-visible spectra of the extracts were as follows: *B1*, λ_{max} in methanol 243, 286, 334, and 615 nm; *R1*, λ_{max} in methanol 238, 290, 363, and 543 nm. *E*, presence of B1 and R1 in untreated fresh human urine. 100 ml of fresh urine was concentrated with a Sep-Pak C_{18} cartridge and fractionated by HPLC. Ligand activity of each 1-min fraction was tested in the yeast AhR assay.

and R1 were also present in untreated fresh human urine, and the dominant AhR ligand in human urine was R1.

R1 was extracted from 120 liters of acid-treated urine and purified by HPLC (see "Experimental Procedures"), yielding about 0.3 mg of pure R1. The electron impact mass spectrum of R1 exhibited a molecular ion peak at *m/z* 262 and two fragment ion peaks at *m/z* 205 and 234 (Fig. 2*A*). Subsequent high resolution mass spectrometry indicated the molecular formula to be $C_{16}H_{10}N_2O_2$ (molecular weight = 262.0740, calculated as 262.0742). Fig. 2*B* shows the presence of 10 protons in the molecule as indicated by the ^1H NMR spectrum of R1 in deuterated dimethyl sulfoxide. This is in agreement with the data

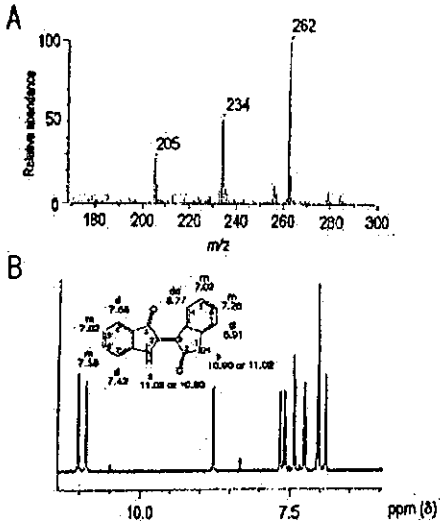

FIG. 2. **Electron impact mass spectrum (*A*) and ^{1}H NMR spectrum (*B*) of R1 and the chemical structure of R1 (indirubin).** Mass spectrum was measured with a JEOL JMS-SX102A spectrometer. ^{1}H NMR spectrum was recorded with a JNM-GSX400 spectrometer in deuterated dimethyl sulfoxide using tetramethylsilane as an internal standard. The structure of R1 was identified as indirubin (17) by ^{1}H NMR and high resolution mass spectroscopy: ^{1}H NMR (Me_2SO-d_6) δ, 11.02 (*s*) and 10.90 (*s*; NH and N'H), 8.77 (*dd*; H-4), 7.66 (*d*; H-4'), 7.58 (*m*; H-6'), 7.42 (*d*; H-7'), 7.26 (*m*; H-6), 7.02 (*m*; H-5 and H-5'), 6.91 (*d*; H-7); J_{4-5} = 7.8, J_{5-6} = 7.8, J_{6-7} = 7.8, $J_{4'-5'}$ = 7.6, $J_{5'-6'}$ = 8.2, $J_{6'-7'}$ = 8.1 Hz; HR-MS *m/z*, 262.0740 and calculated for $C_{16}H_{10}N_2O_2$, 262.0742.

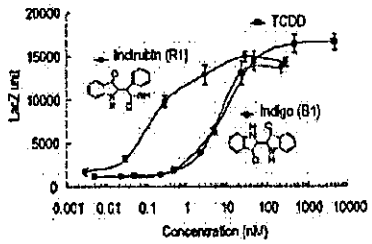

FIG. 3. **AhR ligand activity of indirubin, indigo, and TCDD.** AhR ligand activity of indirubin (*closed circles*), indigo (*open circles*), and TCDD (*closed squares*) in terms of the yeast AhR assay. Each datum is the mean ± S.D. of the quadruplicate experiments.

TABLE I
Concentration of indirubin and indigo in human urine

	Sex	Age	Indirubin (nM)	Indigo (nM)
Sample				
1	Male	22	0.25	0.24
2	Male	23	0.03	0.51
3	Male	23	0.43	0.66
4	Male	24	0.15	0.03
5	Male	24	0.24	0
6	Male	24	0.12	0.03
7	Male	25	0.17	0.57
8	Male	27	0.11	0.06
9	Male	30	0.21	0.08
10	Female	25	0.23	0
Average		24.7 ± 2.3	0.19 ± 0.11	0.22 ± 0.26

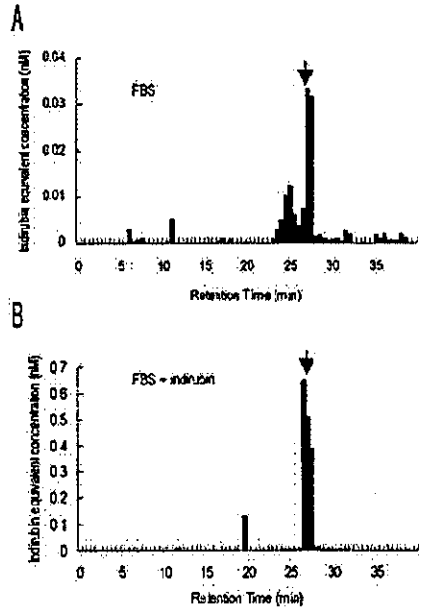

FIG. 4. **Presence of indirubin in FBS.** *A*, 100 ml of FBS was concentrated with a Sep-Pak C_{18} cartridge and resolved by HPLC. AhR ligand activity of each 0.5-min fraction was tested in the yeast AhR assay. *B*, indirubin (0.23 nmol) was spiked into the concentrated FBS before fractionation by HPLC. Indirubin equivalent concentration was calculated from the LacZ units of each fraction and the dose-response curve of indirubin.

from the high resolution mass spectrometry. By ^{1}H NMR and high resolution mass spectroscopy, the structure of R1 was identified as indirubin (17). The HPLC elution profile and the UV-visible absorbance spectrum of synthetic indirubin (14) were identical to those of R1, providing further support for the assignment of R1 as indirubin. Moreover, the HPLC elution profile and the UV spectrum of B1 were identical to those of indigo, which is an isomer of indirubin. We conclude that the major AhR ligands present in the acid-treated human urine are indigo (B1) and indirubin (R1), respectively.

Indigo is one of the oldest dyes known to mankind and has been used since the Bronze Age (~4000 B.C.). Indigo is the dark blue pigment used to dye the denim of blue jeans and other fabrics and is produced by fermentation of plant material from *Isatis tinctoria*, *Indigofera tinctoria*, and *Polygonum tinctorium*. Indirubin is a common pink colored by-product of indigo synthesis (17). Fig. 3 shows the AhR ligand activity of pure indirubin and indigo in the yeast AhR assay. The EC_{50} values of indirubin, indigo, and TCDD were 0.2, 5, and 9 nM, respectively. It is surprising that the activity of indigo was as strong as that of TCDD. More surprisingly, indirubin was ~ 50 times more potent than TCDD as a ligand in the yeast assay. The relative potencies of indirubin and indigo in the yeast AhR assay are reasonable based on the reported K_d values of 12 and 2 nM, respectively, that were determined in AhR ligand binding assays using rat liver cytosol (18). No data regarding the binding affinity of indirubin and indigo are presently available for the human AhR, which was used in our yeast assays.

Indirubin and indigo have been found in the urine of patients with acute myelomonocytic leukemia, porphyrinuria, and purple urine bag syndrome (19, 20), but they have never been reported in urine from normal donors until now. We measured the concentrations of indirubin and indigo in urine that was processed within 15 min after excretion to minimize the potential effects of bacterial action (21). Table I shows that indirubin and indigo are both normally present in human urine at average concentrations of ~0.2 nM. The concentration of indirubin corresponded to the expected value estimated from Fig. 1*B* and Fig. 3.

We also measured the concentrations of indirubin and indigo in FBS. FBS was concentrated by using a Sep-Pak C_{18} cartridge, fractionated every 0.5 min by HPLC and then each fraction was tested by yeast AhR assay (Fig. 4). Two major peaks were observed. According to their retention time, one

was identified as indirubin, but the other was unknown. Indigo was not detected. Indirubin was present at the concentration of 0.07 nM and accounted for half of the total AhR activity of the FBS. The endogenous production of the indirubin and indigo in the human body was expected by the previous works from Gillam *et al.* (17, 22). They found that human cytochrome P450s 2A6, 2C19, and 2E1 catalyzed the formation of indoxyl and isatin from indole, which could then undergo dimerization to form indigo and indirubin.

In Fig. 1*B*, we showed that treatment of urine with sulfuric acid dramatically raised the yields of the ligand activity. Two possible precursors of the active ligand(s) are the sulfate conjugates of indoxyl and isatin. It is possible that these compounds condense to form indigo and indirubin after sufuric acid treatment. Conjugates of indirubin and indigo are also candidates as precursors of the active ligand(s). Although the sulfate conjugate of indoxyl (indican) is a well known component of urine, we presently do not have any information about the concentrations of istatin, indigo, and indirubin conjugates in urine or serum. However, the glucuronidase-treatment experiment suggests that a considerable portion of the ligands in urine exist as glucuronides. Future studies will be directed toward understanding the nature and concentrations of the ligand precursor(s) in urine and serum, as well as the intracellular concentrations, conjugation status, and bioactivity of indigo and indirubin in cells and tissues.

Because the levels of indirubin in human urine and FBS were high enough to activate the AhR, we suspect that indirubin is an endogenous activator of AhR and may play a regulatory role *in vivo*. Indirubin may act to regulate cellular proliferation. Indirubin-mediated activation of AhR may produce an arrest in the G_1 phase of the cell cycle via inhibition of retinoblastoma protein phosphorylation (23, 24) and by transcriptional induction of $p27^{Kip1}$, an inhibitor of CDK4,6-cyclin D1 and CDK2-cyclin E (25). Interestingly, indirubin also inhibits several CDKs and other kinases directly (14). Thus, indirubin levels may control the cell cycle via the AhR pathway and by indirect and direct inhibition of the CDK pathway. Although further studies are needed to clarify the role of indirubin in these pathways, the indirubin concentrations required for AhR activation appear to be lower than those needed to inhibit kinase activity. Thus, the dominant regulatory pathway may be because of indirubin-AhR interactions.

In conclusion, we have identified two potent endogenous AhR ligands, indigo and indirubin, from human urine and bovine serum. Given their potency as ligands and their concentration in human urine and FBS, we propose that these AhR ligands play several important regulatory roles in cells. Further study of these endogenous ligands may reveal the physiological role(s) of AhR and further our understanding of the toxic xenobiotics such as TCDD. Finally, the coupling of yeast reporter assays analogous to the one above with fractionation and analytical characterization of biological materials, such as urine, can provide a fruitful methodology for uniting parental ligands with their orphan receptors.

REFERENCES

1. Pohjanvirta, R., and Tuomisto, J. (1994) *Pharmacol. Rev.* **46**, 483–549
2. Gonzalez, F. J., and Fernandez-Salguero, P. (1998) *Drug Metab. Dispos.* **12**, 1194–1198
3. Okey, A. B., Riddick, D. S., and Harper, P. A. (1994) *Trends Pharmacol. Sci.* **15**, 226–232
4. Huff, J., Lucier, G., and Tritscher, A. (1994) *Annu. Rev. Pharmacol. Toxicol.* **34**, 343–372
5. Hankinson, O. (1995) *Annu. Rev. Pharmacol. Toxicol.* **35**, 307–340
6. Sogawa, K., and Fujii-Kuriyama, Y. (1997) *J. Biochem. (Tokyo)* **122**, 1075–1079
7. Chen, Y.-H., Riby, J., Srivastava, P., Bartholomew, J., Denison, M., and Bjeldanes, L.,. (1995) *J. Biol. Chem.* **270**, 22548–22555
8. Miller, C. A. (1997) *J. Biol. Chem.* **272**, 32834–32829
9. Wei, Y.-D., Helleberg, H., Rannug, U., and Rannug A. (1998) *Chem. Biol. Interact.* **110**, 39–55
10. Sinal, C. J., and Bend, J. R. (1997) *Mol. Pharmacol.* **52**, 590–599
11. Savouret, J.-F., Antenos, M., Quesne, M., Xu, J., Milgrom, E., and Casper, R. F. (2001) *J. Biol. Chem.* **276**, 3054–3059
12. Schaladach, C. M., Riby, J., and Bjeldanes, L. F. (1999) *Biochemistry* **38**, 7594–7600
13. Reiners, J. J., Jr., Clift, R., and Mathieu, R. (1999) *Carcinogenesis* **20**, 1561–1566
14. Hoessel, R., Leclerc, S., Endicott, J. A., Nobel, M. E. M., Lawrie, A., Tunnah, P., Leost, M., Damiens, E., Marie, D., Marko, D., Niederberger, E., Tang, W., Eisenbrand, G., and Meijer, L. (1999) *Nat. Cell Biol.* **1**, 60–67
15. Miller, C. A. (1999) *Toxicol. Appl. Pharmacol.* **160**, 297–303
16. Hayatsu, H. (1992) *J. Chromatogr.* **597**, 37–56
17. Gillam, E. M. J., Notley, L. M., Cai, H., De Voss, J. J., and Guengerich F. P. (2000) *Biochemistry* **39**, 13817–13824
18. Rannug, U., Bramstedt, H., and Nilsson U. (1992) *Mutat. Res.* **282**, 219–225
19. Blanz, J., Ehninger, G., and Zeller K. P. (1989) *Res. Commun. Chem. Pathol. Pharmacol.* **64**, 145–156
20. Jackson, A. H., Jenkins, R. T., Grinstein, M., Ferramola de Sancovich, A. M., and Sancovich, H. A. (1988) *Clin. Chim. Acta* **15**, 245–252
21. Sapira, J. D., Somani, S., Shapiro, A. P., Scheib, E. T., and Reihl, W. (1971) *Metabolism* **20**, 474–486
22. Gillam, E. M. J., Aguinaldo, A. M. A., Notley, L. M., Kim, D., Mundkowski, R. G., Volkov, A. A., Arnold, F. H., Souek, P., DeVoss, J. J., and Guengerich, F. P. (1999) *Biochem. Biophys. Res. Comm.* **265**, 469–472
23. Ge, N.-L., and Elferink, C. J. (1998) *J. Biol. Chem.* **273**, 22708–22713
24. Puga, A., Barnes, S. J., Dalton, T. P., Chang, C.-Y., Knudsen, E. S., and Maier, M. A. (2000) *J. Biol. Chem.* **275**, 2943–2950
25. Kolluri, S. K., Weiss, C., Koff, A., and Gottlicher M. (1999) *Genes Dev.* **13**, 1742–1753

British Journal of Cancer (2000) 83(11), 1488–1494
© 2000 Cancer Research Campaign
doi: 10.1054/ bjoc.2000.1463, available online at http://www.idealibrary.com on IDEAL®

Progesterone receptor isoforms A and B in human epithelial ovarian carcinoma: immunohistochemical and RT-PCR studies

J Akahira[1,2], T Inoue[1], T Suzuki[1], K Ito[2], R Konno[2], S Sato[2], T Moriya[1], K Okamura[2], A Yajima[2] and H Sasano[1]

Departments of [1]Pathology, and [2]Obstetrics and Gynecology, Tohoku University School of Medicine, Sendai, Japan

Summary Human epithelial ovarian carcinoma is well-known as a sex steroid-dependent neoplasm, but the possible biological significance of progesterone receptor (PR) in this cancer remains controversial. Recently, two isoforms of human PR, PRA and PRB, have been characterized and different functional characteristics have been reported for these two isoforms. We therefore examined immunohistochemistry (107 cases) and reverse transcription-polymerase chain reaction (RT-PCR) (16 cases) for PRA, PRB, and oestrogen receptor-a (ER-a). Labeling indices (LI) for PRA and PRB were 2.4 and 43.6, respectively, and the difference was statistically significant. PRB LI, but not PRA LI, as well as performance status, stage, and residual tumour turned out to be independent prognostic factors following multivariate analysis. There was also a significant correlation between ER-a LI and PRB LI ($r = 0.595$, $P < 0.0001$), suggestive of a possible interaction between these two receptors. RT-PCR also detected the expression of PR isoform transcripts in the same pattern as was observed with immunohistochemistry. Results of these studies indicate that PRA and PRB both mediate distinct pathways of progesterone action in ovarian carcinoma. Moreover, it is important to examine PRB LI as a prognostic factor in the cases of human epithelial ovarian carcinoma. © 2000 Cancer Research Campaign http://www.bjcancer.com

Keywords: progesterone receptor; PRA; PRB; ovarian cancer; RT-PCR; immunohistochemistry

Epithelial ovarian carcinoma is the leading cause of death from gynaecological malignancies in the great majority of developed countries (Nakashima et al, 1990). This high mortality is considered to be, in large part, due to the advanced stage of the disease commonly present at the time of diagnosis, but many clinical studies have reported that there are some prognostic factors in ovarian carcinoma other than clinical stages, such as histology, the degree of primary surgical cytoreduction, response to chemotherapy, and others (Young et al, 1978; Redman et al, 1986; Heintz et al, 1986; Piver et al, 1988; Onura et al, 1991; Del Campo et al, 1994).

Sex steroid hormones have been implicated in the aetiology and/or progression of some epithelial ovarian cancers. Both progesterone (PR) and oestrogen receptors (ER) have been reported in human epithelial ovarian carcinoma (Rao and Slotman, 1991). In endometrioid endometrial and breast carcinoma, steroid hormone receptor status correlates well with response to hormonal manipulation and prognosis (McGuire et al, 1978; Benraad et al, 1980; Bloom et al, 1980; Osborne et al, 1980; Ehrlich et al, 1981; Kaupilla, 1984). However, in epithelial ovarian carcinoma, the prognostic significance of tumour ER and PR status among patients still remains controversial (Bizzi et al, 1988; Masood et al, 1989; Sevelda et al, 1990; Rao and Slotman, 1991; Hempling et al, 1998).

PR is a member of a subgroup of nuclear receptors which regulate a number of physiological and morphological processes in response to binding of their ligands (Evans, 1988). There are two isoforms of the human PR, PRA and PRB, which differ only in that the smaller isoform, PRA, lacks the N-terminal 164 amino acids of the larger isoform, PR-B (Horwitz and Alexander, 1983; Jeltsch et al, 1986; Savouret et al, 1990; Kastner et al, 1990). PRA and PRB are products of a single gene and are translated from an individual messenger RNA species under the control of distinct promoters (Kastner et al, 1990). The transcription of both isoforms is indirectly induced by oestradiol via ER (Kastner et al, 1990). Both PRA and PRB function as ligand-activated transcription factors but several in vitro studies have demonstrated different functional characteristics between these two isoforms. For instance, transcriptional activation of the progesterone responsive element-containing promoters by PRB is more marked than that by PRA, although the differences are cell-specific (Kastner et al, 1990; Wen et al, 1994; Giangrande et al, 1997). In addition, PRA can also act as a transcriptional inhibitor of other steroid hormone receptors, including ER and PRB (Wen et al, 1994; Giangrande et al, 1997; Vegeto et al, 1993; Kraus et al, 1995). Results of these studies indicate that the relative levels of PRA and PRB within target cells may determine the nature and functional responses to progesterone.

In the normal human endometrium (Mote et al, 1999; Critchley et al, 1998; Mangal et al, 1997; Wang et al, 1998), leiomyoma (Viville et al, 1997; Fujimoto et al, 1998) and endometrial carcinoma (Kumar et al, 1998; Fujimoto et al, 1995) several studies have examined the relative abundance of PRA and PRB expression, and all studies to date support the presence of distinct pathways of progesterone actions in these tissues. However, the expression of PRA and PRB in epithelial ovarian cancer and their clinical significance have not been examined. Therefore, in this

Received 27 March 2000
Revised 17 July 2000
Accepted 18 July 2000

Correspondence to: J Akahira

Table 1 Correlations between clinical characteristics and hormone receptor immunoreactivity

		Median labelling indices (range)			
	n	PRAB	PRA	PRB	ER[b]
Total[a]	107	42.4 (0–100)	2.4 (0–58.4)	43.6 (0–93.2)	12.8 (0–85.2)
Age					
< 50 years	47	44 (0–100)	4 (0–58.4)	47.2 (0–92)	12.8 (0–85.2)
≥ 50 years	60	41.6 (0–96)	2.2 (0–48)	40.2 (0–93.2)	12.4 (0–63.6)
Performance status					
0–1	76	47.6 (0–100)	2.7 (0–58.4)	45.6 (0–93.2)	16.2 (0–85.2)
2–4	31	30 (0–90)	0 (0–35.2)	25.2 (0–90)	4 (0–63.6)
Histology					
Serous	46	52.8 (0–100)	2.4 (0–43.2)	51.2 (0–93.2)	22.4 (0–85.2)
Endometrioid	18	40 (0–82)	0 (0–52)	39.2 (0–75.6)	0 (0–49.6)
Clear cell	25	32.4 (0–94)	0 (0–35.2)	31.2 (0–92)	8.8 (0–54)
Mucinous	18	55.8 (0–100)	7.4 (0–58.4)	39.7 (0–82)	23.4 (0–67.2)
Stage					
I–II	50	47.4 (0–100)	3 (0–58.4)	43.2 (0–92)	16.2 (0–67.2)
III–IV	57	34 (0–100)	2.4 (0–52)	43.6 (0–93.2)	10.4 (0–85.2)
Grade					
1	44	51.2 (0–100)	2.6 (0–52)	43.6 (0–92)	8.8 (0–68)
2	40	42.4 (0–100)	2.4 (0–58.4)	43.6 (0–90)	14.2 (0–54)
3	23	39.8 (0–96)	0 (0–35.2)	38.8 (0–93.2)	14 (0–85.2)
Residual tumour					
Optimal	77	48 (0–100)	4 (0–58.4)	45.6 (0–92)	14.8 (0–85.2)
Suboptimal	29	27.4 (0–96)	0 (0–31.2)	24 (0–93.2)	4.4 (0–59.2)

[a]Difference of total labelling indices (LI) between PRA and PRB is significant ($P < 0.01$); [b]Significant difference of LIs was observed for performance status and histology ($P < 0.05$); Performance status score: 0 = asymptomatic and fully active; 1 = symptomatic, fully ambulatory, restricted in physically strenuous activity; 2 = symptomatic, ambulatory, capable of self-care, more than 50% of waking hours are spent out of bed; 3 = symptomatic, limited self-care, spends more than 50% of time in bed, but not bedridden; 4 = completely disabled, no self-care, bedridden

study, we evaluated the expression of PRA and PRB in human epithelial ovarian carcinoma using immunohistochemistry and RT-PCR, and their significance as prognostic indicators in epithelial ovarian cancer. We also evaluated the relationship between PR isoforms and ER-α immunohistochemically, because of the unique in vitro activation–inhibition interactions of these sex steroid receptors described above.

MATERIALS AND METHODS

We studied a total of 107 cases of common epithelial ovarian carcinoma. The clinicopathological features of the patients examined are summarized in Table 1. Information regarding age, performance status on admission, histology, stage, grade, residual tumour after primary surgery, response to primary chemotherapy, and overall survival was retrieved from the review of patient charts. Median follow-up time of the patients in this study was 54 months (18–112 months). Seventy-seven patients (71.9%) were optimally cytoreduced at the time of surgery. The great majority of patients (83.2%) received platinum-containing chemotherapy, and approximately half of them (49.4%) received chemotherapy consisting of cisplatin, adriamycin and cyclophosphamide (CAP). Moreover, more than half of the patients (62.5%) who had measurable disease after primary surgery responded to chemotherapy. It was difficult to evaluate the response to primary chemotherapy in relation to survival because 75 of the 107 patients (72.0%) were optimally cytoreduced with primary surgery, and thus they could not be evaluated (NE) on their response to chemotherapy. Performance status was defined according to WHO criteria (World Health Organization, 1979). Histology, stage and grade were determined according to FIGO criteria (International Federation of Gynecology and Obstetrics, 1987; Pettersson, 1994). Residual disease was determined by the amount of unresectable tumour left following primary cytoreductive surgery. Optimal cytoreduction was defined as no gross residual tumour greater than 2 cm in diameter, whereas suboptimal cytoreduction was defined as any gross residual . disease remaining greater than 2 cm in diameter. Response to primary chemotherapy was assessed according to WHO criteria (World Health Organization, 1979). Overall survival was calculated from the time of initial surgery to death, or the date of last contact. Survival times of patients still alive or lost to follow up were censored in February 2000. All of these archival specimens were retrieved from the surgical pathology files at Tohoku University Hospital, Sendai, and Miyagi Prefectural Cancer Center, Natori, Japan. These specimens were all fixed in 10% formalin and embedded in paraffin. Among these 107 cases, 16 cases were available for examination by reverse transcription-polymerase chain reaction (RT-PCR) analysis. These specimens were dissected immediately into small pieces following gross dissection, quickly transferred to liquid nitrogen, and then stored at –80°C until further use. The research protocol was approved by the ethics committee of Tohoku University School of Medicine, Sendai, Japan.

Immunohistochemistry

Immunohistochemical analysis was performed using the streptavidin–biotin amplification method using a Histofine Kit (Nichirei, Tokyo, Japan), and have been previously described in detail (Hirasawa et al, 1997). The characteristics of the primary antibodies employed in this study are summarized in Table 2. The hPRa2 and hPRa3 antibodies recognize PRB and PRA and B, respectively. The hPRa7 antibody employed in this study recognizes both PRA and PRB on immunoblot analysis (Clarke et al,

Table 2 Primary antibodies employed in immunohistochemistry

Antibody	Source	Optimal dilution	Antibody retrieval
PRA and B: hPRa3 (Monoclonal)	Neomarkers (California, USA)	1:50	Autoclave[a]
PR A: hPRa7 (Monoclonal)	Neomarkers (California, USA)	1:100	Autoclave[a]
PRB: hPRa2 (Monoclonal)	Neomarkers (California, USA)	1:100	Autoclave[a]
ER α (Monoclonal)	Immunotech (Marseille, France	1:5	Autoclave[a]

[a]Heat in an autoclave for 5 min in citric acid buffer (2 mM citric acid and 9 mM trisodium citrate dehydrate, pH 6.0)

1987), but specifically recognizes PRA when utilized for immunohistochemistry (Mote et al, 1999). The ER antibody recognizes ER-α, the traditinal estrogen receptor, but not ER-β. The antigen–antibody complex was visualized with 3,3′-diaminobenzidine (DAB) solution (1 mM DAB, 50 mM Tris-HCl buffer, pH 7.6, and 0.006% H_2O_2), and counterstained with haematoxylin. Proliferative-phase endometrial glands were used as positive controls for PR isoforms and ER-α (Clarke et al, 1987). As negative controls, 0.01 M phosphate buffered saline and normal mouse IgG were used in place of primary antibodies. No specific immunoreactivity was detected in these tissue sections.

Scoring of Immunostaining

For evaluation of PRA, PRB, PRAB and ER-α immunoreactivity, labeling index (LI) was obtained in carcinoma cells as described by Sasano et al (1996). We obtained LI in the following manner. Two of the authors (JA and TM) independently evaluated at least 500 carcinoma cells microscopically. These fields of evaluation were determined by these two authors prior to evaluation using double-headed light microscopy. The mean value was obtained when interobserver differences were less than 5%. Immunostained slides were simultaneously evaluated using double-headed light microscopy when interobserver differences were greater than 5%. Intraobserver differences were less than 5% in this study.

RT-PCR

Total RNA was extracted by homogenizing tissue specimens in guanidinium thiocyanate followed by ultracentrifugation in caesium chloride, as described previously (Sambrook et al, 7.1–7.87), and quantified spectrophotometrically at 260 nm. An RT-PCR kit (SUPERSCRIPT Preamplification system, Gibco-BRL, Grand Island NY, USA) was employed in the synthesis and amplification of cDNA. cDNAs were synthesized from 5 μg of total RNA using oligo (dT) primer and reverse transcription was carried out for 50 min at 42°C with SUPERSCRIPT II reverse transcriptase. After an initial 1 min denaturation step at 94°C, 35-cycle PCRs were carried out on a DNA thermal cycler (PTC-200 DNA Engine, MJ Research Inc, USA) under the following conditions: 1 min denaturation at 94°C, 1 min annealing at 56°C, and a 2 min extension at 72°C. Primers for PCR reactions were as follows; PRB (Kumar et al, 1998): 5′ sense-ACAGAATTCATGACTGAGCTGAAGGCAAAGGGT and 3′ antisense-ACAAGATCTCAAACAGGCACCAAGAGCTGCTGA (744–1173, 429 bp); PRAB (Kumar et al, 1998): 5′ sense-ACAGAATTCA TGAGCCGGTCCGGGTGCAAG and 3′ antisense-ACAAGATCTCCACCCAGAGCCCGAGGT TT (1239–1482, 243 bp); β-actin (Willey et al, 1998): 5′ sense-GATTCCTATGTGGGCGACGAG and 3′ antisense-CCATCTCTTGCTCGAAGTCC (192–723, 532 bp). β-actin primers were utilized as positive controls. Negative controls without RNA and without reverse transcriptase were also performed.

Statistical analysis

Statistical analysis was performed using Stat View 5.0 (SAS Institute Inc, North Carolina, USA) software. The statistical significance of association between hormone-receptor status and characteristics of the patients was evaluated using a Mann–Whitney U-test, Kruskal–Wallis, and Scheffe analysis. Correlation among scored PR isoforms and ER-α immunohistochemistry was also assessed using a Spearman rank correlation. Univariate analysis of prognostic significance for prognostic factors was performed using a log-rank test, after each survival curve was obtained by the Kaplan–Meier method. Multivariate analysis of survival time was performed with Cox's proportional hazards model. All patients who could be assessed were included in the intention-to-treat analysis. A result was considered significant when the P value was less than 0.05.

RESULTS

Results of immunohistochemistry are summarized in Table 1. Immunoreactivity for PR isoforms and ER-α were confined exclusively to the nuclei of tumour cells. No immunoreactivity, however, was detected in stromal cells (Figure 1). Median LI for PRB was 43.2% (range 0–93.2%), while that of PRA was 2.4% (0–58.4%). In all histological types and age groups, PRB LI was significantly higher than PRA LI ($P < 0.01$). No significant correlations were detected between PRAB, PRA or PRB LI and any of the clinicopathological parameters in the patients examined in this study. There was a highly significant correlation between ER-α and PRB LI ($r_s = 0.60$, $P < 0.0001$), and a weak correlation was also detected between ER-α and PRA LI ($r_s = 0.28$, $P = 0.038$, Figure 2).

Results of univariate analysis of prognostic significance for each variable, with respect to survival, are summarized in Table 3. In this analysis, we determined the positive cases as those with an LI of more than 10%. There were 35.5% and 71.9% PRA- and PRB-positive cases, respectively. Among the clinicopathological factors examined, those significantly associated with overall survival were histology, stage, performance status, residual tumour, PRAB, PRB, and ER-α immunoreactivity. In multivariate

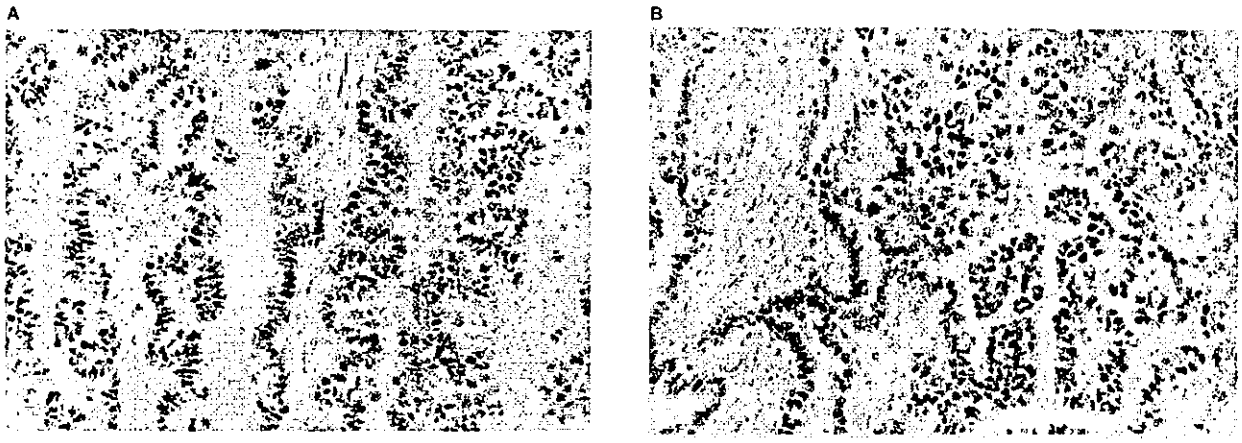

Figure 1 Immunohistochemistry for (A) PRAB and (B) PRB in ovarian serous adenocarcinoma obtained from a 47-year-old patient, stage IIIc. Marked nuclear immunoreactivity was detected for PRAB (A) and PRB (B) in this case (magnification x 200)

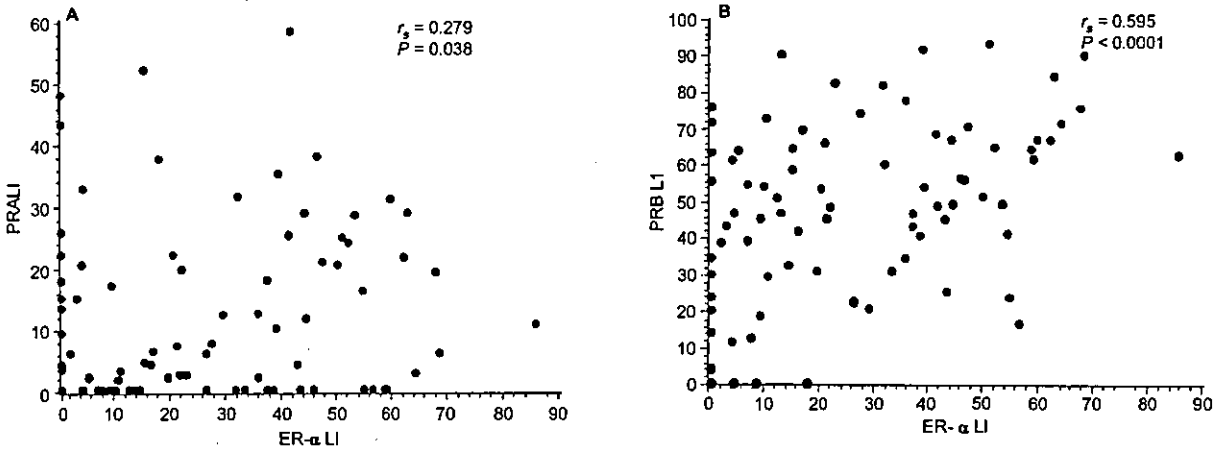

Figure 2 Correlation between (A) PRA and (B) PRB labeling index (LI) and ERα LI in ovarian cancers. Both PR isoforms and ER-α LI were compared by the Spearman rank correlation test. Several points in the Figures (A and B) overlap each other because of the same values

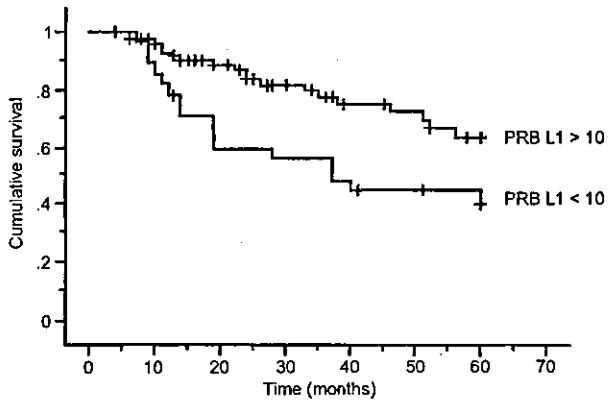

Figure 3 Correlation between PRB labelling index (LI) and survival of patients with epithelial ovarian carcinoma. PRB LI was determined as described in the 'Materials and Methods'. Kaplan–Meier curves were compared

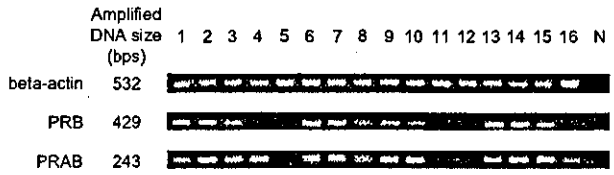

Figure 4 RT-PCR analysis of total RNA extracted from ovarian epithelial carcinoma cases. Bands of the correct size for PRAB (243 bp) and PRB (429 bp) were detected in each histological subtype of ovarian epithelial carcinoma (Lanes 1–5 = serous: lanes 6–8 = mucinous; lanes 9–11 = endometrioid; lanes 12–16 = clear cell). Positive (β-actin) and negative (N) controls are also shown.

analysis, PRB immunoreactivity was a significant (P = 0.037) predictor of overall survival but not PRAB or ER-α (Table 4, Figure 3). Performance status, stage, and residual tumour all turned out to be independent prognostic factors. Results of RT-PCR analysis for each histologic subtype are summarized in Figure 4. The expression of the mRNAs for PRAB and PRB are: serous, 4/5 and 3/5; mucinous, 3/3 and 3/3; endometrioid, 2/3 and

Table 3 Univariate analysis of overall survival

Factor	n	Median survival (months)	P
Age			
< 50 years	47	> 60	0.9
≥ 50 years	60	56	
Performance status			
0–1	76	> 60	< 0.0001
2–4	31	22	
Histology			
Serous	46	60	0.0375[a]
Endometrioid	18	37	
Mucinous	18	> 60	
Clear cell	25	> 60	
Stage			
I–II	50	> 60	< 0.0001
III–IV	57	38	
Grade			
1	44	> 60	0.504
2	40	51	
3	23	35	
Residual disease after primary surgery			
Optimal	77	> 60	< 0.0001
Suboptimal	29	19	
PRAB LI			
Negative	28	40	0.0207
Positive	79	> 60	
PRA LI			
Negative	69	> 60	0.24
Positive	38	> 60	
PRB LI			
Negative	30	37	0.0117
Positive	77	> 60	
ER-αLI			
Negative	51	52	0.0374
Positive	56	> 60	

[a]Significant difference was observed for endometrioid vs mucinous adenocarcinoma; positive immunoreactivity was defined as LI > 10

2/3; clear cell, 4/5 and 3/5, respectively. The positivities of RT-PCR analysis in each case of ovarian carcinoma were consistent with those of immunohistochemistry.

DISCUSSION

Human epithelial ovarian carcinoma is believed to be a sex steroid hormone-dependent neoplasm, but the biological significance of PR, especially its role in growth regulation, and its correlation to clinical outcome in patients, has remained in dispute. Several groups of investigators reported no significant difference in the survival of ovarian cancer patients with respect to PR levels (Bizzi et al, 1988; Geisler et al, 1996; Masood et al, 1989), while some other studies have reported that a higher PR status correlated well with increased survival (Inversen et al, 1986; Masood et al, 1989; Slotman et al, 1989; Kommoss et al, 1992; Hempling et al, 1998; Langdon et al, 1998). Review of these reports indicates that the difference in these studies may be due to the heterologous composition of the patient population. For example, several groups of investigators included tumours of low malignant potential and others included only cases with advanced stage of cancer (Masood et al, 1989; Geisler et al, 1996; Hempling et al, 1998). Hempling et al (1998) and Inversen et al (1986) both demonstrated PR as a significant prognostic factor following multivariate analysis, but both examined only advanced (stage III–IV) epithelial ovarian carcinoma. Therefore, in this study we evaluated only epithelial ovarian carcinoma without low malignant potential, in all stages and all major histologic subtypes using a multivariate analysis.

Table 4 Multivariate analysis of survival time using Cox's proportional hazards model

Covariate	Relative risk	95% CI[a]	P
Performance status			
0–1	1.000		
2–4	2.907	1.242–6.803	0.0138
Histology			
Serous	1.000		
Endometrioid	2.162	0.821–5.698	0.119
Clear cell	1.659	0.655–3.788	0.177
Mucinous	0.423	0.044–4.082	0.457
Stage			
I–II	1.000		
III–IV	2.565	1.252–10.222	0.028
Residual disease after primary surgery			
Optimal	1.000		
Suboptimal	5.150	2.000–13.333	<0.001
PRAB LI			
Negative	1.000		
Positive	0.210	0.039–1.126	0.069
PRB LI			
Negative	1.000		
Positive	0.173	0.0333–0.901	0.037
ER LI			
Negative	1.000		
Positive	0.878	0.316–2.440	0.802

[a]CI = confidence interval

The identification of PR subtypes demonstrates that the analysis of subtypes for PR can provide new insights into the biological roles of PR in human epithelial ovarian carcinoma. In our study, PRB is dominantly expressed in all types or groups of epithelial ovarian carcinoma using both immunohistochemistry and RT-PCR. In addition, PRB, but not PRAB, immunoreactivity turned out to be an independent prognostic factor following multivariate analysis. In all previous studies on PR in ovarian epithelial carcinoma, PR isoforms were not evaluated separately as in PRAB in our present study. Therefore, the discrepancy between the results of previous studies and our present examination may be due to the evaluation of PR subtype in our study, and the analysis of PR isoforms considered important in the evaluation of the survival of patients diagnosed with epithelial ovarian carcinoma. Fujimoto et al (1995) reported the expression of PR isoform mRNAs in ovarian carcinoma using RT-PCR. In their study, six out of ten cases expressed only PRB mRNA. They subsequently concluded that the dominancy of PRB mRNA expression was associated with the advanced clinical stage of ovarian cancer (Fujimoto et al, 1995). Results of their study, especially the dominance of PRB, but not PRA mRNA, were consistent with those of our present study (Fujimoto et al, 1995). Therefore, the dominant expression of PRB is considered to be a characteristic feature of ovarian cancer, in contrast to breast and endometrial carcinoma, in which PRA is the dominant subtype of PR (Kumar et al, 1998; Graham et al, 1996).

The biological role of progesterone in epithelial ovarian carcinoma is unknown, but progesterone is, in general, considered to function antagonistically to oestrogen-mediated cell proliferation (Clarke and Sutherland, 1990). PRA has been reported to be a transcriptional inhibitor of ER (Simpson et al, 1998), and PRB has the ability to up-regulate the transcription of genes required for cell differentiation (Kumar et al, 1998). The transcriptional activation of PRB is more marked than PRA (Kastner et al, 1990), which

suggests that the inhibitory effects on cell proliferation by progesterone is, at least, initially mediated through PRB.

Friedlander et al (1989) described a significantly lower S-phase fraction among PR-positive tumours compared with PR-negative tumours. Additionally, they demonstrated that a significantly greater proportion of diploid tumors were PR-positive than were aneuploid tumours (Friedlander et al, 1989). Both tumour ploidy and proliferative activity, determined by S-phase fraction, have been demonstrated to be significant determinants in the survival of patients with epithelial ovarian cancer (Erhardt et al, 1984; Volm et al, 1985). Therefore, ovarian epithelial carcinoma cases associated with functional PR, especially PRB, and sufficient in situ availability of progesterone are considered to be associated with better clinical outcome. This may be due to the inhibitory actions of progesterone on tumour cell proliferation, but this hypothesis awaits further investigation for clarification. Kumar et al (1998) examined the expression of PRA and PRB in endometrial carcinoma and reported that selective down-regulation of PRB may represent an insufficient response to progestin therapy in patients with poorly differentiated endometrial carcinoma (Kumar et al, 1998). Similar results were also reported in breast carcinoma, i.e. tumours containing primarily PRA related to poor response to endocrine agents (Geisler et al, 1996). These studies have demonstrated that the dominant expression of PRB suggests a good response for progestin in breast and endometrial cancer patients, although the clinical usefulness of sex steroid hormones in the treatment of ovarian cancer has yet to be determined (Ahlgren et al, 1993).

There was, in general, a good correlation between ER-α and PR in epithelial ovarian carcinoma, suggesting that the regulation of PR, especially of PRB, may be under oestrogen control in ovarian epithelial carcinoma, consistent with the results of previous in vitro studies (Kastner et al, 1990; Savouret et al, 1990). Both PRA and PRB mRNAs have been demonstrated to be increased by oestrogen, but between these two isoforms, preferential up-regulation of PRB by oestrogen has been reported in the T47D human breast carcinoma cell line (Graham et al, 1995), and in human endometrial tissue (Mangal et al, 1997). However, it has also been reported that the stimulatory effects of oestrogen on PRA protein levels were greater than PRB in chicken oviduct (Syvala et al, 1997), suggesting that oestrogen stimulation of PRA and PRB is likely to be cell-, tissue-, and species-specific. In addition, mechanisms other than those under ER control can influence PR expression, as was demonstrated in PR-positive, ER-negative breast tumours (Horwitz, 1981). PR expression has been demonstrated to be regulated by growth factors (Katzenellenbogen and Norman, 1990), and ER-α knockout mice continue to express a low level of PR mRNA (Shughrue et al, 1997). Therefore, further investigations are required to clarify the possible mechanisms of regulation of PRA and PRB in human epithelial ovarian carcinoma.

ACKNOWLEDGEMENTS

This work is in part supported by the grant-in-aid for Cancer Research 7–1 from the Ministry of Health and Welfare, Japan, a grant-in-aid for scientific research area on priority area (A-11137301) from the Ministry of Education, Science and Culture, Japan, a grant-in-aid for Scientific Research (B-11470047) from Japan Society for the Promotion of Science and a grant from The Naitou Foundation and Suzuken Memorial Foundation. We appreciate Dr Toru Tase and Dr Hiroo Tateno for their cooperation in retrieving the specimens of ovarian carcinoma tissues at the Miyagi Prefectural Cancer center, Natori, Japan. We also appreciate Ms Keiko Abe and Ms Ayako Kusumi for their technical assistance. We would like to acknowledge the editing of the manuscript by Mr Andrew D Darnel, Department of Pathology, Tohoku University School of Medicine, Sendai, Japan.

REFERENCES

Ahlgren JD, Ellison NM, Gottlieb RJ, Laluna F, Lokich JJ, Sinclair PR, Ueno W, Wampler GL, Yeung KY, Alt D and Fryer JG (1993) Hormonal palliation of chemoresistant ovarian cancer: three consecutive Phase II trials of the Mid-Atlantic Oncology Program. *J Clin Oncol* **11**: 1957–1968

Benraad THJ, Friberg CG, Koenders AJM and Kullander S (1980) Do estrogen and progesterone receptors (ER and PR) in metastasizing endometrial cancer predict response to estrogen therapy. *Acta Obstet Gynecol Scand* **59**: 155–159

Bizzi A, Codegoni AM and Landoni F (1988) Steroid receptors in epithelial ovarian cancer: Relation to clinical parameters and survival. *Cancer Res* **48**: 6222–6226

Bloom ND, Tobin EH, Schreiberman B and Degenshein GA (1980) The role of progesterone receptors in the treatment of breast cancer. *Cancer Res* **45**: 2992–2997

Clarke CL and Sutherland RL (1990) Progestin regulation of cellular proliferation. *Endocr Rev* **11**: 266–301

Clarke CL, Zaino PD, Feil PD, Miller JV, Steck ME, Ohlsson-Wilhelm BM and Satyaswaroop PG (1987) Monoclonal antibodies to human progesterone receptor: Characterization by biochemical and immunohistochemical techniques. *Endocrinology* **121**: 1123–1132

Critchley HOD, Wang H, Kelly RW, Gebbie AE and Glasier AF (1998) Progestin receptor isoforms and prostaglandin dehydrogenase in the endometrium of women using a levonorgestrel-releasing intrauterine system. *Hum Reprod* **13**: 1210–1217

Del Campo JM, Felip E, Rubio D, Vidal R, Bermejo B, Colomer R and Zanon V (1994) Long-term survival in advanced ovarian cancer after cytoreduction and chemotherapy treatment. *Gynecol Oncol* **53**: 27–32

Ehrlich CE, Young PLM and Cleary RE (1981) Cytoplasmic progesterone and estradiol receptors in normal, hyperplastic and carcinomatous endometria: Therapeutic implications. *Am J Obstet Gynecol* **141**: 539–546

Erhardt K, Aver G, Bjorkholm E, Forsslund G, Moberger B, Silfversward C, Wicksell G and Zetterberg A (1984) Prognostic significance of DNA content in serous ovarian tumors. *Cancer Res* **44**: 2198–2202

Evans RM (1988) The steroid and thyroid hormone receptor superfamily. *Science* **240**: 889–895

Friedlander M, Quinn MA, Fontune D, Foo MS, Toppila M, Hudson CN and Russell P (1989) The relationship of steroid receptor expression to nuclear DNA distribution and clinicopathologic characteristics in epithelial ovarian tumors. *Gynecol Oncol* **32**: 184–190

Fujimoto J, Ichigo S, Hori M, Nishigaki M and Tamaya T (1995) Expression of progesterone receptor form A and B mRNAs in gynecologic malignant tumors. *Tumor Biol* **16**: 254–260

Fujimoto J, Hirose R, Ichigo S, Sakaguchi H, Li Y and Tamaya T (1998) Expression of progesterone receptor form A and B mRNAs in uterine leiomyoma. *Tumor Biol* **19**: 126–131

Geisler JP, Wiemann MC, Miller GA and Geisler HE (1996) Estrogen and progesterone receptor status as prognostic indicators in patients with optimally cytoreduced stage IIIc serous cystadenocarcinoma of the ovary. *Gynecol Oncol* **60**: 424–427

Giangrande PH, Pollio G and McDonnell DP (1997) Mapping and characterization of the functional domains responsible for the differential activity of the A and B isoforms of the human progesterone receptor. *J Biol Chem* **272**: 32889–32900

Graham JD, Roman SD, McGowan EM, Sutherland RL and Clarke CL (1995) Preferential stimulation of human progesterone receptor B expression by estrogen in T47D human breast cancer cell lines. *J Biol Chem* **270**: 30693–30700

Graham JD, Yeates C, Balleine RL, Harvey SS, Milliken JS, Bilous AM and Clarke CL (1996) Progesterone receptor A and B protein expression in human breast cancer. *J Steroid Biochem Mol Biol* **56**: 93–98

Heintz APM, Hacker NF, Berek JS, Rose TP, Munoz AK and Lagasse LD (1986) Cytoreductive surgery in ovarian carcinoma: Feasibility and morbidity. *Obstet Gynecol* **67**: 783–788